

Spatio-temporal changes in extreme sea levels along the coasts of the North Atlantic and the Gulf of Mexico

Marta Marcos^{1,2} 

¹ IMEDEA (UIB-CSIC), Miquel Marqués 21, 07190 Esporles, Balearic Islands, Spain

² Department of Physics, University of the Balearic Islands, Cra. Valldemossa, km 7.5, Palma, Spain

Philip L. Woodworth³ 

³ National Oceanography Centre, Joseph Proudman Building, 6 Brownlow Street, Liverpool L3 5DA, United Kingdom

Abstract

Extreme sea levels along the densely monitored coasts of the North Atlantic Ocean and the Gulf of Mexico have been investigated using high frequency tide gauge measurements in the GESLA-2 data set (www.gesla.org). Our results, based on non-tidal residuals and skew surges in records since 1960, confirm that mean sea level (MSL) is a major, but not a unique, driver of extremes. Regionally-coherent linear trends and correlations with large scale climate patterns are found in extreme events, even after the removal of MSL. A similar conclusion, that MSL is a major but not the only driver of extremes, comes from a small number of long records starting in the mid-19th century. The records show slight increases in the intensity of extreme episodes at centennial time scales, together with multi-decadal variability unrelated to MSL. Objective statistical criteria have been used to investigate whether extreme sea level distributions are stationary or not, resulting in non-stationarity being favoured in many records, with or without accounting for changes in MSL. Extremes have been found to favour a non-Gumbel behaviour at many locations, with implications for the accuracy of return levels for coastal engineering.

1. Introduction

Increases in annual mean and extreme sea levels are recognised as being one of the consequences of climate change (Church et al., 2013). The two parameters are known to vary to a similar extent at many locations, when annual values are investigated over several decades, suggesting that the variability and trends in extreme sea levels are largely determined by changes in mean sea level (MSL) (Woodworth et al., 2011 and references therein). However, this simple relationship does not apply at some stations, or during sections of some station records, which means that there is more to be understood about this topic.

In this paper, we make use of tide gauge records from the relatively data-rich coastlines of the North Atlantic and Gulf of Mexico in order to learn more about the relationships

between changes in MSL and extreme sea levels, and between changes in MSL and the differences between this version and the Version of Record. Please cite this article as doi: 10.1002/2017JC013065

non-tidal contributions to the extremes. We represent the latter in two ways. The first way uses non-tidal residuals, obtained from conventional tidal analyses of tide gauge data, while the second way makes use of values of skew surges. A skew surge is defined as the difference between the maximum sea level occurring around each astronomical high tide minus the astronomical high tide level itself (Pugh and Woodworth, 2014). It had application first in the Dutch storm surge warning system (de Vries et al., 1995) and is often a more useful indicator of ‘surge magnitude’ than the conventional non-tidal residuals (Williams et al., 2016). Skew surge is a well-defined quantity in the predominantly semi-diurnal tidal regimes which occur around most of our coastlines. Skew surges have an additional advantage over non-tidal residuals in being a more suitable parameter for study of extremes when using tide gauge data with poor timing.

The ocean tide is a major contributor to individual extreme events at some locations (Merrifield et al., 2013). In addition, there are known to be small changes in the ocean tide at some locations on North Atlantic coastlines, which are poorly understood (e.g. Ray, 2009). Therefore, small contributions from tidal changes to changes in extreme sea levels over several decades can be anticipated. However, we do not consider such tidal changes to be a major complicating consideration in the present study.

In addition to forming an overall impression of the relationships between MSL and extreme sea levels, and in particular where relationships are weaker than elsewhere, we consider the seasonal dependence of such findings, and the stationarity of findings through the records using modern statistical methods that allow the description of the probability of occurrence of extreme sea levels as a function of climate parameters.

If such studies of MSL and extreme sea levels are to have predictive value, then there has to be some insight into how changes in extremes observed in the past have depended upon the various forcings responsible for them, and into how such forcings may change in the future. For example, it may be relevant to consider the relationship between extreme sea levels and the main climate index for the region (the North Atlantic Oscillation, NAO) and how it might change in the future.

2. Data and methods

2.1 GESLA-2 data selection and processing

We have used the Global Extreme Sea Level Analysis (GESLA) tide gauge data set (Woodworth et al., 2017). The recently released version (GESLA-2) consists of 1355 globally distributed tide gauge records sampled at hourly or higher frequencies. We have selected three of the most densely monitored regions that also boast some of the longest tide gauge records, namely the European Atlantic coasts, including the North and Baltic Seas (containing 203 stations), the North American Atlantic coasts (85 stations) and the Gulf of Mexico (35 stations). See Figure 1 for their spatial distribution.

For our studies of annual MSL and extreme sea levels, we have restricted our analyses to the period starting 1960, when the number of stations increases significantly (Holgate

et al., 2013). This selection, and a requirement for each record to have at least 25 years of data, reduces the total number of stations from 323 to 207 records (24 of these station records are from stations with more than one record, arising from contributions to GESLA by more than one data provider. We have checked as far as possible that alternative records at each station provide similar information on extremes below). For studies of winter extreme levels, we required 25 years of good data starting in October 1959; for summers, we required 25 years starting in June 1960.

In addition, we made use of 7 of the longest tide gauge records in GESLA-2 with lengths over 100 years. These records, which have been analysed over their complete length, have been chosen as representative of different areas. Finally, high waters recorded in Liverpool from the mid-19th century have also been considered for the study of the multi-decadal changes in extremes, updated from those in Woodworth and Blackman (2002).

The astronomical ocean tides have been computed using the Matlab[®] UTide software package (Codiga, 2011). The last 15 years of data at each station have been used to estimate the tidal constituents, including the annual and the semi-annual signals. One of the advantages of this tool is its ability to extract tidal constituents from a sea level record with data gaps and uneven temporal sampling. The latter is a common feature in many tide gauge records. Requirements for storm surge and tsunami monitoring, and general technical improvements, have resulted in many gauges being upgraded in recent years to higher frequency sampling (IOC, 2016). Time series of the astronomical tide and non-tidal residuals have been obtained by means of the tidal analysis, and skew surges have been computed as described below. MSL was estimated using a Butterworth low-pass filter of order 2 with a cut-off period of 2 years applied to the original observations. MSL defined in this way, therefore, is a continuous function of time. Menéndez and Woodworth (2010), for example, defined mean and median sea levels on a year-by-year basis, and in the present paper we refer to the latter as ‘annual median removal’ (similarly ‘seasonal median removal’ when individual seasons are discussed).

2.2 Percentile studies of observed sea levels

Percentile techniques have been used extensively in studies of extreme sea levels and non-tidal residuals. For example, Menéndez and Woodworth (2010) made use of the first version of the GESLA data set in a quasi-global study of extreme sea levels, with the conclusion that variability and trends in the high percentile annual extremes depended largely upon changes in MSL. They also showed a clear association between MSL and extreme sea levels in their common dependence upon climate indices such as the El Niño – Southern Oscillation (ENSO) or NAO.

In Sections 3 and 4 below, we update such analyses, using the more complete and up-to-date GESLA-2 data set, for annual, winter (October-March) and summer (June-September) percentiles of both total sea levels and their non-tidal residuals, with and without removal of MSL.

In addition to calculating time series of percentiles of total sea levels and non-tidal residuals, we have also calculated time series of the number of hours in each year or season for which sea level exceeds a certain threshold, which in practice we define to be the overall 99th or 99.9th percentiles. These time series thereby represent the duration of high water levels over a threshold, rather than the statistics of those levels themselves. The importance of changes in MSL to the significance of trends in these duration time series can similarly be estimated by including MSL in, or removing MSL from, the original record.

2.3 Skew surge computation

Historical sea level records sometimes contain timing errors (time shifts or drifts) which impact on the tidal analysis, resulting in an imperfect separation of tidal and non-tidal components. Such timing errors manifest themselves as large tidal oscillations in the non-tidal residual time series, and have the greatest importance where the tides are themselves large. One way to avoid the problem is to perform a detailed quality control and remove the periods when timing errors are identified (e.g. Thompson et al., 2013; Marcos et al., 2015). This is a time-consuming process and implies a significant reduction in the amount of useable data.

An alternative approach is to use skew surges instead of non-tidal residuals. The skew surge is the difference between the maximum water height and the predicted tidal high water level within a tidal cycle. (In principle, one could also study skew surges at low as well as high waters. For present purposes, we have focused on those at high waters only for comparison to findings on extreme high waters from total water levels.) The following method efficiently determines the skew surges in any tidal regime. The first step consists in finding the maxima and minima of sea level using the time derivative of the measured sea level curve. Maxima are selected on the basis of zeros in a decreasing time derivative. For each maximum occurring at time t_i we define its tidal cycle as the period starting half-way between t_i and the previous maximum t_{i-1} , and half-way between t_i and the next maximum t_{i+1} . Finally, the skew surges are computed for each tidal cycle as the difference between the observed maximum and the highest astronomical tide level. This is done only when there are no data gaps in the time series during the tidal cycle. As a result, a quasi-global data set of skew surges has been computed and made available via the website www.gesla.org, not only for North Atlantic and Gulf of Mexico coasts, but for all 1355 tide gauge records in GESLA-2.

It is important to note that the astronomical tide used in the computation of the skew surges does not include MSL, so any variation in MSL (inter-annual variability or long-term trend) will manifest itself in the skew surge value.

The time series of skew surges have been used to derive their annual and seasonal (winter and summer) percentiles, in a similar way to the derivation of percentiles of total water level described above. The impact of MSL changes on the skew surges has been assessed in two different ways. The first one consists in removing the MSL using the low-pass filtered time series of observations at the time of occurrence of each

individual skew surge. In the second one, the 50th percentile (median) of the skew surges has been subtracted from the higher order percentiles on an annual or seasonal basis.

Extreme skew surge ‘events’ have been defined either as those episodes exceeding the overall 95th, 99th and 99.9th percentiles of the skew surge time series, or the highest values per year or season, depending on the analyses to be carried out. To ensure independence, a separation of 72 h between two consecutive events has been required. For each extreme skew surge event, we have estimated its persistence. The duration of the skew surge event cannot be estimated from the skew surge itself as, by definition, the skew surge occurs once for each tidal cycle, unlike the time series of total water levels. Therefore, the persistence must be computed with respect to a predefined threshold which is taken from observed sea level time series. In our case, the number of hours over the 95th and 99th percentiles of observed sea level has been calculated for the highest skew surges.

2.4 Extreme value distributions of skew surges

The five largest independent skew surges per year at each station have been selected to characterise their extreme value distributions. The optimal number of extreme skew surges per year has been chosen after applying a multiplier score test (Bader et al., 2016). This test provides a sequential measure of the goodness-of-fit of the r -largest block maxima that is objective and robust. The obtained value of $r=5$ is in agreement with earlier assessments (e.g. Marcos et al., 2015).

The r -largest Generalized Extreme Value (GEV) distribution (Coles, 2001) has been fitted to the empirical datasets at each station using maximum likelihood estimation and $r=5$. The estimated parameters μ (location), σ (scale) and ξ (shape) were then used to compute the M -year return levels. The shape parameter controls the tail behaviour of the distribution and determines whether the return levels have an asymptotic limit (when $\xi < 0$) or are unbounded (when $\xi > 0$) (e.g. Coles, 2001). In the special case when $\xi = 0$, the extreme level is proportional to the logarithm of return period and the distribution is known as a Gumbel distribution.

Earlier works have demonstrated the non-stationary nature of extreme sea levels at the global (Menéndez and Woodworth, 2010) and regional scales (Marcos et al., 2009; Cid et al., 2015) even after the removal of MSL (Talke et al., 2014; Wahl and Chambers, 2015; Marcos et al., 2015). Here we have explored changes in the r -largest GEV distributions using a parametric approach in which the location parameter is allowed to vary linearly with time and with large scale climate indices. The shape parameter has been demonstrated to remain unchanged in studies of other climate parameters (Davison and Ramesh, 2000), and we follow Marcos et al. (2015) who pointed out that temporal variations in the scale parameter of extreme sea levels worldwide were negligible. The assumption of stationarity has been checked using the Akaike Information Criterion (AIC; Akaike, 1974) between the stationary and different non-stationary models. The AIC is a quantitative measure of the quality of the fit of the theoretical model weighted

by its complexity (i.e. the number of parameters). It will be used to define the preferred model (stationary or not) for a given station before and after the removal of MSL. Other possibilities, such as the Bayesian Information Criterion, have also been checked and led to very similar results.

All the methods described in this section have been implemented in R using the R package “eva” (Bader and Yan, 2015) available at https://github.com/geekman1/eva_package.

3. Long term trends in sea level extremes

3.1 Observed sea level extremes

Linear trends of annual and seasonal sea level 99th percentiles since 1960 are mapped in Figure 2. The equivalent maps for the 99.9th percentile are shown in Figure S1. We recall here that only stations with at least 25 years of data have been used. Results for total sea levels (Figure 2, upper row) mimic the MSL trends and the well-known spatial pattern of Glacial Isostatic Adjustment (GIA) in Scandinavia. Trends are significant at 70% of the stations for the annual percentiles, and similar in the seasonal cases; the significance of a trend is defined at the 95% confidence level. When the annual or seasonal median is removed from the observations (Figure 2, middle row) the trends become non-significant in the majority of the stations; however about 23% of the stations still present significant linear changes of annual 99th percentiles. The same applies for the winter season, which shows similarities also in the sign and magnitude of the trends. Conversely, during the summer, trends are statistically significant in only roughly 10% of the stations. Indeed, annual trends in the 99th percentile of total sea levels after median removal are mostly determined by winter trends (42 stations determined by significant winter trends compared to 16 stations by summer trends). If non-tidal residuals are used instead of total sea levels (Figure 2, bottom row), the number of stations with significant trends remains similar, although the actual trend values change at most sites. Overall, these results are in agreement with Menéndez and Woodworth (2010) in terms of the sign of the linear trends and the reduction of the significant stations when the observations and non-tidal residuals are median reduced. Likewise, Mawdsley and Haigh (2016) also found mostly negative trends for the 99th percentile of non-tidal residuals (which were similarly defined so as to not include MSL variations) along the Atlantic coast of southern Europe, where these were significant, and small and negative trends in the northernmost stations of the US Atlantic coast. The exact match in the trends is not expected due to the different periods considered.

In addition to the magnitudes of the extremes, also their durations are relevant and have been explored. Figure 3 represents the linear trends in the number of hours above the 99th and the 99.9th percentiles computed over the entire period since 1960. The durations increase along with MSL (Figure 3, upper row); when the excess over the 99.9th percentile is considered (Figure 3c), the number of hours is often too small to provide significant trends (see for example the non-significant values in the Gulf of Bothnia). Note the different colour scales when the two thresholds are used. After the removal of

MSL (note again that we removed the low-passed total sea level, not the yearly median), significant changes in the duration of extremes over the 99th percentile are still found in 76 stations (36% out of the total), of which 63 display positive trends (Figure 3b). A similar picture is found when the threshold is increased up to the 99.9th percentile (Figure 3d), although the number of stations with significant trends is reduced in accordance with the smaller number of values above the higher threshold.

3.2 Skew surges

The time-averaged characteristics of the skew surges for the period 1960-onwards are illustrated in Figure 4. Maximum skew surges (Figure 4a) range from only 17 cm at low latitudes of the Northeast Atlantic up to 4 m in the North Sea, whereas median skew surges vary within ± 15 cm (Figure 4b). The number of skew surges per year is spatially highly variable (Figure 4c). The skew surges per year have been estimated here as those independent (i.e. separated by at least 72 h) skew surge events that exceed a given threshold (in our case defined as the 99th percentile of the overall skew surge time series). The median values of the number of skew surges range between only 1 (e.g. in the Baltic Sea) and up to 8 events per year, with the mean of all stations being 3.5 events per year. For each of these events, their persistence has been computed as the number of hours around the timing of the event in which sea level was above a predefined threshold. Note that this threshold is not the same as the threshold used to define the events. Here we have used the 99th percentile of total sea levels, which resulted in the mean persistence of skew surges mapped in Figure 4d. The average duration of an extreme skew surge event is less than 5 hours in about 50% of the stations. Notably, in some areas, such as the Baltic Sea, the mean duration exceeds 20 hours, lasting therefore for more than two tidal cycles (however, those tidal cycles are small in the case of the Baltic).

Temporal changes in skew surges have been explored in the same way as for total sea levels and non-tidal residuals. Linear trends for the annual and seasonal 99th percentiles are mapped in Figure 5. Figure S2 represents the results for the 99.9th percentiles. The spatial patterns of trends in skew surges (Figure 5, upper row) follow, once again, the linear trends in MSL and thus are very similar to those obtained for total sea level for the annual and seasonal cases. Whereas the percentage of stations with statistically significant trends of skew surge percentiles range between 60-70%, it is reduced to 6-15% when MSL is removed (Figure 5, middle row). The comparison with Figure 2 confirms that percentiles of total sea level and skew surges present the same behaviour in terms of spatial patterns and trends, in line with earlier works (e.g. Dangendorf et al., 2014; Mawdsley and Haigh, 2016).

The impact of MSL removal in general has also been addressed by removing the annual and seasonal medians of the skew surges (Figure 5, middle row) instead of the low-pass filter removal. The resulting trends are very similar to those obtained when MSL is removed (Figure 5, bottom row). The skew surges with MSL and with median removal show an average correlation of 0.94 and an average bias of only 1 cm (being at most 3

cm in the North Sea). Since the median of the skew surges contains the inter-annual changes associated with MSL together with changes in storminess, these results indicate that inter-annual changes in MSL are much larger than inter-annual changes in surges.

In the following, the impact of MSL in skew surges is accounted for on the basis of the low-pass filtered total sea levels. Linear trends in the number of skew surge events that exceed the 99th percentile are mapped in Figure 6 for annual and seasonal cases. The yearly number of events increases significantly at most sites where relative MSL is rising and decreases where relative MSL is dropping (in the Baltic Sea) (Figure 6a). The same applies for winter (Figure 6c), the season during which most of the extreme events occur at mid-latitudes. In summer, however, the changes are non-significant at 85% of the stations, due to the low occurrence of extremes (Figure 6e). After the removal of MSL, trends are still significant in 42 (40) stations for the annual (winter) series (Figure 6b,d). The number of extreme skew surges per year unrelated to MSL changes shows positive trends at the Atlantic stations of the British Isles and in northern France as well as along the coasts of the Gulf of Mexico. Similar conclusions are reached when the threshold is increased to the 99.9th percentile (Figure S3). While the evidence for positive trends in the Gulf of Mexico is reduced to only one station being statistically significant, the number of stations with positive trends is enhanced along the North American coast. Unlike the changes in the number of extreme skew surges, the duration of these events does not display significant trends at most stations (Figure 7). The trend in the duration of the extreme skew surge events is significant and negative along the eastern Baltic Sea (Figure 7a), but this spatial feature almost entirely disappears when MSL is removed (Figure 7b). This finding is consistent with the results when total sea levels are used (Figure 3). However, the overall values of the trends in the persistence of the skew surges are one order of magnitude smaller than those of total sea levels. The patterns shown in Figure 7 are the same when the threshold to determine the duration is lowered to the 95th percentile (not shown).

4. Links with large scale climate indices

Variations of sea level extremes at inter-annual and decadal time scales have been related to large scale atmospheric patterns in the past (Menéndez and Woodworth, 2010; Marcos et al., 2009; Talke et al., 2014; Marcos et al., 2015; Mawdsley and Haigh 2016, Wahl and Chambers, 2016). We therefore computed the linear (Pearson) correlations between the high order percentiles and a selected set of climate indices downloaded from the Global Climate Observing System (GCOS) Working Group on Surface Pressure website and available at http://www.esrl.noaa.gov/psd/gcos_wgsp/Timeseries/. These indices are the North Atlantic Oscillation (NAO), the Arctic Oscillation (AO), two indices used to describe El Niño Southern Oscillation (NIÑO3 and the Southern Oscillation Index, SOI) and the Atlantic Multidecadal Oscillation (observed AMO).

The correlations of the annual and seasonal 99th percentiles of sea level and the NAO are mapped in Figure 8 before and after the removal of MSL. Statistically significant correlations of NAO with annual percentiles are found along all the investigated coasts

(Figure 8a), with positive values in Northern Europe and negative southwards and along the North American and Gulf coasts. These correlations remain at most sites (62 out of 89) even after MSL removal (Figure 8d), indicating that the influence of the NAO is not only limited to the MSL. The same holds for the winter season (Figure 8b,e). During winter, the impact of the NAO is larger in the North Sea, but is smaller along the southern latitudes of the North American coast. The impact of the NAO is smaller during summer (Figure 8c,f), with the only exception being in the Gulf of Mexico and parts of the American Atlantic coast where slightly negative correlations can be observed. All the above also applies when the 99th percentiles of skew surges are correlated with NAO (Figure S4).

The resulting correlations between skew surges 99th percentiles and AO (Figure S5) have the same pattern as those from NAO, as expected since AO and NAO are also correlated with each other. The influence of the AO is larger at the high latitudes. In contrast with the NAO, negative correlations after MSL removal can be identified with summer percentiles along the western Baltic Sea coast. Correlations with the indices describing El Niño (Figures S6 and S7) show that the impact of the Southern Oscillation can be detected along the North American coast during the winter season, regardless of whether MSL has been removed or not. Finally, the AMO does correlate significantly with the 99th skew surges percentiles, although its influence is mostly through the MSL changes (Figure S8)

5. Extreme value distributions

An important question in extreme sea level analysis is whether the distributions of extremes are better described by a full GEV parameterisation, or by a restricted Gumbel description in which the shape parameter is set to zero.

We have fitted GEV and Gumbel distributions to the GESLA-2 records, using the five largest skew surges per year after the removal of MSL, assuming stationarity in location, scale and shape parameters (Figure 9). Again, only those stations with at least 25 years of valid data since 1960 have been used. According to AIC, only in ~27% of the stations is the Gumbel fit preferred to the GEV (Figure 9a). These stations are distributed primarily in the North Sea and along the North American coast. At those stations for which GEV is preferred, the shape parameter ranges between -0.3 and 0.3 (Figure 9b), with the largest negative values located along the Atlantic European coasts and positive values in the Canary Islands, Gulf of Mexico and at low latitudes along the North American coast. The geographical coherence of the shape parameter provides, on the one hand, confidence in the obtained values (an important issue given that GESLA-2 data have not been quality controlled beyond that already undertaken by the data providers); and, on the other hand, can be interpreted as an indicator of distinct extreme regimes. Indeed, when the shape parameter is estimated using only winter or only summer extreme episodes (not shown) the differences between the European and North American coastlines are enhanced. In particular, during the summer season the shape parameter in the Gulf of Mexico reaches its maximum values of up to 0.3, consistent

with the fact that in this region extremes are dominated by tropical cyclones occurring in summer (see also Tebaldi et al., 2012). Nevertheless, positive shape parameters may arise as an artefact of inadequate sampling of the rare events from tropical cyclones.

The associated 50-year return levels are mapped in Figure 9c. The largest return levels, exceeding 4 m, are found in the North Sea while the lowest are located in low-latitude European stations. Return levels along the Atlantic North American coasts and the Gulf of Mexico are comparable in magnitude to those for the Atlantic north European stations, with values between 1 and 2 m. In contrast, when return levels are computed for the summer events (not shown), the larger values, around 1.5 m, are found in the Gulf of Mexico and the North Sea, whereas they are around 50 cm elsewhere. In the North Sea, a closer look at synoptic wind patterns reveals that these values are associated with perturbations travelling eastwards and generating strong zonal winds. Likewise, winter return levels do not exceed 50 cm in the Gulf of Mexico, in agreement with the fact that the extreme events are caused by summer cyclones in this region.

The results above suggest that assuming zero shape parameter (i.e. Gumbel-like distributions) may have important implications regarding the return level assessment. Extremes are often assumed to have a Gumbel-like distribution (e.g. the extremes in total water level discussed by Hunter et al., 2013). However, the differences in 50-year return levels for skew surges when using a GEV and a Gumbel distribution are shown in Figure 9d. Using a Gumbel distribution, and an assumption that the GEV is more correct, it overestimates the 50-year return levels by more than 70 cm in the North Sea and British Isles stations, and underestimates by up to 30 cm the return levels along the coasts of the Gulf of Mexico.

5.1 Time-varying extreme distributions

The assumption of stationarity of the extreme value distribution of skew surges does not necessarily hold, especially when MSL is included in the skew surge definition. To investigate the possibility of non-stationarity, we have fitted the GEV distribution to the five largest annual skew surges since 1960, allowing for temporal variations in the location parameter, μ . We have then tested the similarity of the results of these fits to those of the stationary case on the basis of the AIC values. When the MSL is included in the time series, the non-stationarity prevails, with 77% of the stations being better described with a linear trend in the location parameter. The values of these trends are mapped in Figure 10a. When MSL is removed, the number of stations for which the non-stationary distribution is preferred is reduced to 40%, but there are still regions where coherent linear trends are found (Figure 10c), such as those located in the Atlantic European coasts.

Non-stationary skew surges distribution is also more suitable than the stationary case when the location parameter is allowed to vary linearly with the NAO, both before (Figure 10b) and after (Figure 10d) MSL removal. In this case, the non-stationary stations are 28% and 43% before and after removing MSL, respectively. There is, therefore, a clear impact of the NAO in inter-annual changes of extreme skew surges

unrelated to MSL. Likewise, when other climate indices are used, there is also dependence in the extreme distribution. If the AO is considered (Figure S9a,c), results are comparable to the NAO, with large coherent regions in Europe. If NIÑO3 is used (Figure S9b,d) the influence is constrained to the North American and Gulf of Mexico coasts and mostly through its impact on MSL.

6. Lessons from the longest tide gauge records

The non-stationary behaviour of the extreme sea levels raises the question of to what extent the results for the period 1960 onwards, shown above, hold at longer time scales. Earlier works have already detected evidence of multi-decadal variability in non-tidal residuals (Marcos et al., 2015) and skew surges (Mawdsley and Haigh, 2016). Here, we have investigated the long term behaviour of extreme skew surges at multi-decadal to centennial time scales using a selection of long tide gauge records distributed in different extreme regimes. These stations are Brest, Cuxhaven, Stockholm, Halifax, New York, Key West and Galveston, representative of the European Atlantic, North Sea, Baltic Sea, Atlantic North America, Tropical Atlantic North America and the Gulf of Mexico, respectively. In addition, high water values in Liverpool since 1846 (Woodworth and Blackman, 2002) have also been included in the analysis, updated to 2014 using more recent data. For Liverpool, the skew surges were computed by subtracting tidal predictions (that include the seasonal constituents as above) from high waters. To account for the impact of MSL in Liverpool we have used the annual or seasonal median of the skew surges, since the low-pass filtered series is not available in this station, as the early years of Liverpool information were derived from high and low waters rather than regularly sampled sea levels, and both approaches had anyway been shown to provide very similar results elsewhere (see section 3). The Liverpool data used here are from 1846 only for consistency with the other time series; for information on earlier years at this location, see Woodworth and Blackman (2002).

The number of independent skew surges exceeding the overall 99th percentile has been computed for each long record. Given the seasonal differences observed in the skew surges, we have selected the winter extremes in all stations, with the exception of Galveston, where we used the summer values, that being the season when the largest extreme events tend to occur. Nevertheless, yearly values would provide very similar results. In order to enhance the decadal variability the counts were grouped into 5-year bins (Figure 11). Everywhere in the selected set the number of skew surges above the threshold follows MSL changes as implied by Figure 11 (red dots). Thus, the number of extreme surges increases during the 20th century, in agreement with the linear trends in both total and skew surge high order percentiles dominated by MSL (see Figures 2 and 5). The obvious exception is Stockholm where relative MSL drops due to GIA and so does the number of events following MSL removal. After MSL is removed, the frequency of occurrence of extreme skew surges shows decadal changes (Figure 11, blue bars). Note that the thresholds applied to count the number of events with and without MSL are not the same, since they correspond to the percentiles of the series before and after the MSL removal. In Cuxhaven and Stockholm the results indicate an

increased storminess since 1950 with respect to the first half of the 20th century (these are the only two stations with statistically significant linear trends); however, this cannot be extrapolated outside the North Sea and Baltic Sea areas. In particular, the series in Liverpool suggests that the storminess during the last 20 years is comparable to that observed during the late 19th to early 20th centuries.

In a second step, we have fitted a non-stationary GEV distribution to the five annual largest skew surges for the entire period of each series, allowing the location parameter to vary linearly with time and with the NAO. MSL has been removed from all series to focus on changes in the storm surge component. Again, winter extremes have been selected in all stations except in Galveston, where we have used summer maxima. The resulting parameters were applied to compute the time-varying 50-year return level. The five extreme skew surges and the 50-year return levels computed using the entire periods are plotted in Figure 12 (red). For comparison, the 50-year return levels computed using the GEV parameters obtained for extremes after 1960, mapped in Figure 10, are also shown (blue). The resulting return level curves may differ because of the temporal changes in the extreme distributions (last 60 years vs. the last century). Return levels curves during the two periods show the same dependence with the NAO but different linear trends and, in the stations Brest, Halifax, Stockholm and Galveston, also values that are significantly different using 1960-onward only from the long term return levels. Particularly striking is the difference in 50-year return level in Galveston, exceeding 0.5 m due to the fact that the two strongest events occurred after 1960. Differences in the magnitude and even the sign of the trends reflect the multi-decadal variability of extremes, in line with earlier works (e.g. Marcos et al., 2015; Mawdsley and Haigh, 2016). At centennial time scales, Brest shows a slightly negative trend during the whole period of -0.02 ± 0.01 mm/yr; Cuxhaven, Stockholm, Key West and Galveston show statistically significant positive trends in the 50-year return levels, ranging between 0.16 ± 0.12 mm/yr in Key West and 1.48 ± 0.94 mm/yr in Cuxhaven. The result in Cuxhaven is consistent with the positive trends in high order percentiles reported by Dangendorf et al. (2014) for the same period. The latter trend apparently had a contribution from the locally-increasing tide in the second half of the 20th century (Mudersbach et al., 2013). Therefore, our determination of the tide from the last 15 years of data alone (Section 2.1), could have contributed to our positive trend for Cuxhaven in Figure 12.

7. Discussion and Conclusions

Many authors have recognised the importance of changes in MSL to changes in the occurrence of extreme sea levels (Woodworth et al., 2011). For example, as regards the US Atlantic coast, Zhang et al. (2010) were among the first to point out the similarity in both sets of time series. More recently, Wahl and Chambers (2015) concurred with the importance of MSL to changes in extremes on the US coast, but pointed to sections of coast where additional (non-MSL) processes could influence the extremes. These included the southeast coast and the winter season when storm surges are driven by extra-tropical cyclones. In a following paper, Wahl and Chambers (2016) concluded

that much of the variability in extremes can be accounted for by climate indices, which implied predictive capability for future extremes. Links between extreme sea levels, ENSO, NAO and AMO along the US Atlantic and Gulf coasts have been suggested by Kennedy et al. (2007), Park et al. (2010), Sweet and Zervas (2011) and Talke et al. (2014). Wahl et al. (2014) emphasised the importance of the seasonal ‘baseline’ of MSL to the impact of storm surges for the Gulf coast in particular, and thereby of the overall water level. Studies of individual stations have pointed to the importance of MSL changes to extremes (e.g. New York, Talke et al., 2014), and the importance of future changes in MSL to both major and ‘nuisance’ flooding is recognised (Sweet et al., 2013; Sweet and Park, 2014; Ray and Foster, 2016; Vousdoukas et al., 2017). Thompson et al. (2013) used tide gauge data to estimate changes in overall wintertime storminess along US coasts.

In the Mediterranean, Letetrel et al. (2010) used the long tide gauge record from Marseille and attributed long-term changes in extreme sea levels to those in MSL, although with differences from decade to decade, generally confirming findings from other southern European stations (Marcos et al., 2009). In northern Europe, recent comparisons of trends in MSL, and sea level extremes can be found for the English Channel (Haigh et al., 2010), and Newlyn in particular (Bradshaw et al., 2016), and the Baltic (e.g. Suursaar and Sooäär, 2007). Mudersbach et al. (2013) pointed to some periods when changes in MSL and extreme sea levels in the German Bight were roughly the same, and periods when they were not. Some of the variability in European extreme sea levels has been linked to solar cycle (Martínez-Asensio et al., 2016). A review of the subject for Europe in general has been given by Weisse et al. (2014).

The present study of sea level extremes has made use of the largest collection of tide gauge data currently available. Even large tide gauges data sets are known to have limitations regarding spatial sampling, especially when the largest events are considered (Pugh and Woodworth, 2014). That is why we have confined ourselves in the present study to the use of data from the relatively data-rich North Atlantic coastlines only.

We have confirmed the importance of MSL to variability and trends in extreme sea levels along North Atlantic coasts. We have updated findings (e.g. Menéndez and Woodworth, 2010) based on the investigation of total sea levels and non-tidal residuals. We have also made use of skew surges as more reliable indicators of non-tidal sea level storminess (Williams et al., 2016) and corroborated their consistency with non-tidal residuals regarding long term trends and variability. Ours is not the first study to make use of skew surges. Mawdsley and Haigh (2016) used the GESLA-1 data set and focused on the use of either non-tidal residuals or skew surges in determining changes in surge occurrence, finding little evidence for long-term changes in either. They found significant tide-surge interaction at over half the sites studied, again pointing to the value of skew surge as a practical measure of ‘surge’.

Despite the fact that the extreme skew surges are modulated to a large extent by MSL, significant changes in their intensity and frequency still remain after MSL removal. It

must be noted also that changing temporal sampling may result in changes in the accuracy of extremes. However, we find good spatial coherence in both trends and correlations between nearby stations, which would not be the case if some of them were biased. Part of these changes is linked to large scale climate indices, with the NAO being one of the dominants in our region of study. The impact of the NAO is larger during the winter season when the atmospheric mode is also stronger. Its signature is detected consistently in the inter-annual changes of high order percentiles and in the time-varying extreme distributions. Indeed, in the majority of the stations, objective statistical criteria favoured non-stationary extreme distributions, instead of the stationary approach, when linear trends and the NAO are included in the location parameter. This has a number of implications: first, the link between extreme skew surges and large scale climate modes is reflected in a regional consistency of the extremes, as pointed out also by Mawdsley and Haigh (2016) who built regional skew surge indices. Second, it suggests the possibility of using tailored climatic indices that could be more suitable in areas where the NAO or other standard indices may not correlate significantly. In this line, Wahl and Chambers (2016) defined such indices based on atmospheric and ocean variables to explain changes in extreme distributions derived from stationary distributions fitted in sliding time windows. Third, climate indices may have predictable skills for extreme sea levels. For example, the Intergovernmental Panel on Climate Change Fifth Assessment Report (Kirtman et al., 2013, section 11.3.2.4) concluded that there was only medium confidence in near-term projections of a northward shift of Northern Hemisphere storm tracks and westerlies, and thereby increases in the NAO/AO. However, it can be seen from Figure S4(a,d) that, even if there are only small increases in the NAO, that increases in extreme sea levels can be expected in the Baltic region and decreases along the American Atlantic coast, even after accounting for MSL. Predictive skills based on observational evidence may complement other work on modelling extreme projections (e.g. Vousdoukas et al., 2017).

Extreme time series spanning more than 100 years provide a long term context for the interpretation of the reported decadal changes. There are several tide gauge records in GESLA-2 fulfilling this requirement. Using seven of these records, plus Liverpool, representative of different extreme regimes, we have demonstrated that the number of independent extreme events follows MSL; this is probably why the most intense storm seasons are perceived to have occurred during the last two decades (except in Scandinavia where relative MSL has dropped) in which the flooding and impacts were more pronounced. However, after the removal of MSL, there is no evidence of an overall increased storm activity either in Europe or along the North American Atlantic coasts. This contrasts with the results by Wadey et al. (2014) who, on the basis of the Newlyn tide gauge record, concluded that the 2013/14 winter season was particularly unusual due to the clustering of extreme events. Our results on the number of events per winter in Liverpool (and also in Newlyn, not shown here) are consistent with those found by Wadey et al. (2014) in Newlyn back to the start of that record in 1915. But

earlier observations in Liverpool suggest that the number of extremes in the late 19th century was comparable to recent years.

The longest records show that skew surge return levels unrelated to MSL display multi-decadal variations superimposed on centennial trends that are small but predominantly positive during the last 100 years or so. At inter-annual time scales, return levels are also modulated by the NAO in the North Atlantic. This conclusion complements the direct relationship found by Marcos et al. (2015) at multi-decadal time scales. We have also found that the dependence between NAO and return levels remains unchanged, thus supporting predictability of extremes in the long term.

Acknowledgements

The GESLA-2 data set of skew surges referred to in Section 2.3 is available at www.gesla.org. We thank the many providers of tide gauge data to GESLA-2. M. Marcos acknowledges a “Ramon y Cajal” contract funded by the Spanish Ministry of Economy. This work was supported by the Research Project CLIMPACT (CGL2014-54246-C2-1-R, AEI/FEDER, UE) funded by the Spanish Ministry of Economy. This work was undertaken when P. Woodworth was an Honorary Research Fellow at the National Oceanography Centre in Liverpool in receipt of an Emeritus Fellowship from the Leverhulme Trust. Part of this work was funded by UK Natural Environment Research Council National Capability funding. The authors are grateful to Dr. John Hunter for his comments and advice on the manuscript.

References

- Akaike, H. (1974), A new look at the statistical model identification, *IEEE T. Automat. Contr.*, 19 (6), 716–723, doi:10.1109/TAC.1974.1100705.
- Bader, B., J. Yan, and X. Zhang (2016), Automated selection of r for the r largest order statistics approach with adjustment for sequential testing, *Stat. Comput.*, doi:10.1007/s11222-016-9697-3.
- Bader, B., and J. Yan (2016), The eva package, available from https://github.com/geekman1/eva_package.
- Bradshaw, E., P.L. Woodworth, A. Hibbert, L.J. Bradley, D.T. Pugh, C. Fane, and R.M. Bingley (2016), A century of sea level measurements at Newlyn, SW England, *Mar. Geod.*, 39(2), 115-140, doi:10.1080/01490419.2015.1121175.
- Church, J.A., P.U. Clark, A. Cazenave, J.M. Gregory, S. Jevrejeva, A. Levermann, M.A. Merrifield, G.A. Milne, R.S. Nerem, P.D. Nunn, A.J. Payne, W.T. Pfeffer, D. Stammer, and A.S. Unnikrishnan (2013), *Sea Level Change*. In: Stocker, T.F., D. Qin, G.-K. Plattner, M. Tignor, S.K. Allen, J. Boschung, A. Nauels, Y. Xia, V. Bex and P.M. Midgley (eds.), *Climate Change 2013: The Physical Science Basis*. Contribution of

Working Group I to the Fifth Assessment Report of the Intergovernmental Panel on Climate Change. Cambridge University Press, Cambridge, United Kingdom and New York, NY, USA.

Codiga, D.L. (2011), Unified tidal analysis and prediction using the UTide Matlab functions, Technical Report 2011-01, 59 pp., Graduate School of Oceanography, University of Rhode Island, Narragansett. Available from <ftp://www.po.gso.uri.edu/pub/downloads/codiga/pubs/2011Codiga-UTide-Report.pdf>.

Dangendorf, S., S. Muller-Navarra, J. Jensen, F. Schenk, T. Wahl, and R. Weisse (2014), North Sea storminess from a novel storm surge record since AD 1843, *J. Clim.*, 27, 3582–3595, doi:10.1175/JCLI-D-13-00427.1.

Davison, A.C., and N.I. Ramesh (2000), Local likelihood smoothing of sample extremes, *J.R. Stat. Soc. B.*, 62 (1), 191–208.

de Vries, H., M. Breton, T. de Mulder, et al. (1995), A comparison of 2D storm surge models applied to three shallow European seas, *Environ. Softw.*, 10, 23–42, doi:10.1016/0266-9838(95)00003-4.

Haigh, I., R. Nicholls, and N. Wells (2010), Assessing changes in extreme sea levels: Application to the English Channel, 1900-2006, *Cont. Shelf Res.*, 30, 1042-1055, doi:10.1016/j.csr.2010.02.002.

Holgate, S.J., A. Matthews, P.L. Woodworth, L.J. Rickards, M.E. Tamisiea, E. Bradshaw, P.R. Foden, K.M. Gordon, S. Jevrejeva, and J. Pugh (2013), New data systems and products at the Permanent Service for Mean Sea Level, *J. Coastal Res.*, 29, 493-504, doi:10.2112/JCOASTRES-D-12-00175.1.

Hunter, J.R., J.A. Church, N.J. White, and X. Zhang (2013), Towards a global regionally varying allowance for sea-level rise, *Ocean Eng.*, 71, 17-27, doi:10.1016/j.oceaneng.2012.12.041.

IOC (2016), Manual on Sea-level Measurements and Interpretation, Volume V: Radar Gauges. Paris, Intergovernmental Oceanographic Commission of UNESCO. 104pp. (IOC Manuals and Guides No.14, vol. V; JCOMM Technical Report No. 89) (English). Available from <http://unesdoc.unesco.org/images/0024/002469/246981E.pdf> which includes a Supplement: Practical Experiences.

Kennedy, A. J., M. L. Griffin, S. L. Morey, S. R. Smith, and J. J. O'Brien (2007), Effects of El Niño–Southern Oscillation on sea level anomalies along the Gulf of Mexico coast, *J. Geophys. Res.*, 112, C05047, doi:10.1029/2006JC003904.

Kirtman, B., S.B. Power, J.A. Adedoyin, G.J. Boer, R. Bojariu, I. Camilloni, F.J. Doblas-Reyes, A.M. Fiore, M. Kimoto, G.A. Meehl, M. Prather, A. Sarr, C. Schär, R. Sutton, G.J. van Oldenborgh, G. Vecchi, and H.J. Wang (2013), *Near-term Climate Change: Projections and Predictability*. In: Climate Change 2013: The Physical Science Basis. Contribution of Working Group I to the Fifth Assessment Report of the Intergovernmental Panel on Climate Change [Stocker, T.F., D. Qin, G.-K. Plattner, M.

Tignor, S.K. Allen, J. Boschung, A. Nauels, Y. Xia, V. Bex and P.M. Midgley (eds.)]. Cambridge University Press, Cambridge, United Kingdom and New York, NY, USA.

Letetrel, C., M. Marcos, M.B. Martín, and G. Wöppelmann (2010), Sea level extremes in Marseille (NW Mediterranean) during 1885-2008, *Cont. Shelf Res.*, 30, 1267-1274, doi:10.1016/j.csr.2010.04.003.

Marcos, M., M.N. Tsimplis, and A.G.P. Shaw (2009), Sea level extremes in southern Europe, *J. Geophys. Res.*, 114, C01007, doi:10.1029/2008JC004912.

Marcos, M., F.M. Calafat, A. Berihuete, and S. Dangendorf (2015), Long-term variations in global sea level extremes, *J. Geophys. Res. Oceans*, 120, doi:10.1002/2015JC011173.

Martínez-Asensio, A., M.N. Tsimplis, and F.M. Calafat (2016), Decadal variability of European sea level extremes in relation to the solar activity, *Geophys. Res. Lett.*, 43, 11744-11750, doi:10.1002/2016GL071355.

Mawdsley, R.J., and I.D. Haigh (2016), Spatial and temporal variability and long-term trends in skew surges globally, *Front. Mar. Sci.*, 3, 29, doi:10.3389/fmars.2016.00029.

Menéndez, M., and P.L. Woodworth (2010), Changes in extreme high water levels based on a quasi-global tide-gauge dataset, *J. Geophys. Res.*, 115, C10011, doi:10.1029/2009JC005997.

Merrifield, M.A., A.S. Genz, C.P. Kontoes, and J.J. Marra (2013), Annual maximum water levels from tide gauges: Contributing factors and geographic patterns, *J. Geophys. Res.*, 118, 2535-2546, doi:10.1002/jgrc.2017.

Mudersbach, C., T. Wahl, I.D. Haigh, and J. Jensen (2013), Trends in high sea levels of German North Sea gauges compared to regional mean sea level changes, *Cont. Shelf Res.*, 65, 111-120, doi:10.1016/j.csr.2013.06.016.

Park, J., J. Obeysekera, M. Irizarry-Ortiz, J. Barnes, W. Park-Said (2010), Climate Links and Variability of Extreme Sea-Level Events at Key West, Pensacola, and Mayport, Florida, *Journal of Waterway, Port, Coastal, and Ocean Engineering*, 136, 6

Pugh, D.T., and P.L. Woodworth (2014), *Sea-level science: Understanding tides, surges, tsunamis and mean sea-level changes*. Cambridge: Cambridge University Press. ISBN 9781107028197. 408pp.

Ray, R.D. (2009), Secular changes in the solar semidiurnal tide of the western North Atlantic Ocean, *Geophys. Res. Lett.*, 36, L19601, doi:10.1029/2009GL040217.

Ray, R.D., and G. Foster (2016), Future nuisance flooding at Boston caused by astronomical tides alone, *Earth's Future*, 4, doi:10.1002/2016EF000423.

Suursaar, Ü., and J. Sooäär (2007), Decadal variations in mean and extreme sea level values along the Estonian coast of the Baltic Sea, *Tellus A*, 59 (2), 249-260, doi:10.1111/j.1600-0870.2006.00220.x.

Sweet, W.V., and C. Zervas (2011), Cool-season sea level anomalies and storm surges along the U.S. East Coast: Climatology and comparison with the 2009/10 El Niño, *Mon. Weather Rev.*, 139, 2290-2299, doi:10.1175/MWR-D-10-05043.1.

Sweet, W.V., and J. Park (2014), From the extreme to the mean: Acceleration and tipping points of coastal inundation from sea level rise, *Earth's Future*, 2, 579-600, doi:10.1002/2014EF000272.

Sweet, W., C. Zervas, S. Gill, and J. Park (2013), Hurricane Sandy inundation probabilities today and tomorrow. pp. 17-20 in, *Explaining Extreme Events of 2012 from a Climate Perspective* (eds. T.C. Peterson, M.P. Hoerling, P.A. Stott and S. Herring). Bulletin of the American Meteorological Society, 94, S17-S74. Available from www.ametsoc.org/2012extremeeventsclimate.pdf.

Talke, S.A., P. Orton, and D.A. Jay (2014), Increasing storm tides in New York Harbor, 1844-2013, *Geophys. Res. Lett.*, 41, 3149-3155, doi:10.1002/2014GL059574.

Tebaldi, C., B. H. Strauss, C.E. Zervas (2012), Modelling sea level rise impacts on storm surges along US coasts, *Env. Res. Lett.*, doi:10.1088/1748-9326/7/1/014032

Thompson, P.R., G.T. Mitchum, C. Vonesch, and J. Li (2013), Variability of winter storminess in the eastern United States during the twentieth century from tide gauges, *J. Clim.*, 26, 9713-9726, doi:10.1175/JCLI-D-12-00561.1.

Vousdoukas, M. I., L. Mentaschi, E. Voukouvalas, M. Verlaan, and L. Feyen (2017), Extreme sea levels on the rise along Europe's coasts, *Earth's Future*, 5, doi:10.1002/2016EF000505.

Wahl, T., F.M. Calafat, and M.E. Luther (2014), Rapid changes in the seasonal sea level cycle along the US Gulf coast from the late 20th century. *Geophys. Res. Lett.*, 41, 491-498, doi:10.1002/2013GL058777.

Wahl, T., and D.P. Chambers (2015), Evidence for multidecadal variability in US extreme sea level records, *J. Geophys. Res. Oceans*, 120, 1527-1544, doi:10.1002/2014JC010443.

Wahl, T., and D.P. Chambers (2016), Climate controls multidecadal variability in U. S. extreme sea level records, *J. Geophys. Res. Oceans*, 121, 1274-1290, doi:10.1002/2015JC011057.

Weisse, R., D. Bellafiore, M. Menéndez, F. Méndez, R.J. Nicholls, G. Umgiesser, and P. Willems (2014), Changing extreme sea levels along European coasts, *Coast. Eng.*, 87, 4, 4-14, doi:10.1016/j.coastaleng.2013.10.017.

Williams, J., K.J. Horsburgh, J.A. Williams, and R.N.F. Proctor (2016), Tide and skew surge independence: New insights for flood risk, *Geophys. Res. Lett.*, 43, 6410-6417, doi:10.1002/2016GL069522.

Woodworth, P.L., M. Menéndez, and W.R. Gehrels (2011), Evidence for century-timescale acceleration in mean sea levels and for recent changes in extreme sea levels, *Surv. Geophys.*, 32(4-5), 603-618 (erratum page 619), doi:10.1007/s10712-011-9112-8.

Woodworth, P.L., J.R. Hunter, M. Marcos, P. Caldwell, M. Menéndez, and I. Haigh (2017), Towards a global higher-frequency sea level data set, *Geosci. Data J.*, (in press), doi:10.1002/gdj3.42.

Zhang, K.Q., B.C. Douglas, and S.P. Leatherman (2000), Twentieth-century storm activity along the US east coast, *J.Clim.* 13, 1748-1761, doi:10.1175/1520-0442(2000)013<1748:TCSAAT>2.0.CO;2.

Figure Captions

Figure 1. Tide gauge distributions from GESLA-2. Stations with at least 25 years of data for 1960-on (207 stations) are marked in blue and stations spanning a period of at least 75 years (38) in red. Black dots indicate the rest of the stations (111).

Figure 2. Linear trends of annual 99th percentiles of total sea level (a), with median removed (b) and for non-tidal residuals with median removed (c). Panels d-e-f are the same for winter and g-h-i for summer. Black dots indicate non-significant trends at the 95% confidence level.

Figure 3. Trends in the number of hours each year that sea level exceeds the overall 99th (a) and 99.9th (c) percentiles of sea level for the whole record. (b) and (d) are the same but with MSL removed.

Figure 4. Maxima (a) and median (b) skew surges. Median number of skew surges (c) and the duration of their events (d).

Figure 5. Linear trends of annual 99th percentiles of skew surges (a), with median removed (b) and with MSL removed (c). Panels d-e-f are the same for winter and g-h-i for summer. Black dots indicate non-significant trends at the 95% confidence level.

Figure 6. Linear trends of the number of skew surges exceeding the 99th percentile (a) and the same after removing MSL (b). The same for winter in (c,d) and for summer (e,f)

Figure 7. Linear trends of the duration of events with the highest 1% of skew surges each year (over the 99th percentile) with MSL (a) and without MSL (b)

Figure 8. Correlations between NAO and 99th percentiles of total sea level (a) and for winter (b) and summer (c). The same after removing MSL (d,e,f). Black dots indicate non-significant correlations at the 95% confidence level.

Figure 9. a) Skew surge extremes following GEV or Gumbel-like distributions after removing MSL, b) shape parameter for non-Gumbel stations, c) 50-year return periods using a GEV distribution, and d) differences in 50-year return periods between Gumbel and GEV distributions (i.e. Gumbel minus GEV).

Figure 10. a) Linear trend in the location parameter for the non-stationary GEV distribution and the same without MSL (c). NAO dependence of the location parameter (b) and the same after MSL removal (d).

Figure 11. Number of skew surges every five years exceeding the 99th skew surge percentiles for the 8 selected long records, with MSL (red dots) and MSL removed (blue bars). Summer surges are used in Galveston and winter otherwise.

Figure 12. Five largest skew surges per season in selected stations (black dots). Winter values are used everywhere except in Galveston where summer values are represented. In Liverpool, grey dots indicate the skew surges from the current Gladstone tide gauge that has replaced earlier stations. Also plotted are time-varying 50-year return levels with the $1-\sigma$ uncertainties computed using the entire period (red) and since 1960 (blue). Units are m.

Figure S1. As in Figure 2 but for 99.9th percentiles.

Figure S2. As in Figure 5 but for 99.9th percentile

Figure S3. As in Figure 6 but for 99.9th percentile.

Figure S4. As in Figure 8 but for skew surges. Figure S5. As Figure S4 but for AO

Figure S6. As Figure S4 but for NIÑO3

Figure S7. As Figure S4 but for SOI

Figure S8. As Figure S4 but for AMO

Figure S9. AO dependence of the location parameter (a) and the same without MSL (c). NIÑO3 dependence of the location parameter (b) and the same without MSL (d).

Figure 1.

Accepted Article

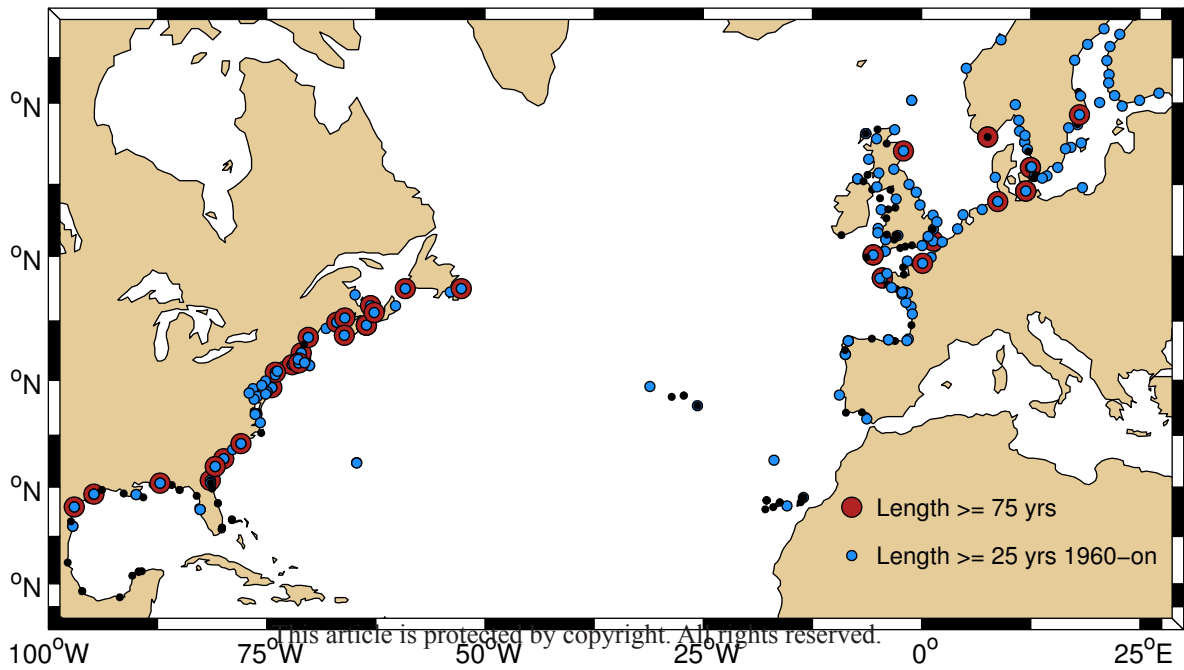


Figure 2.

Accepted Article

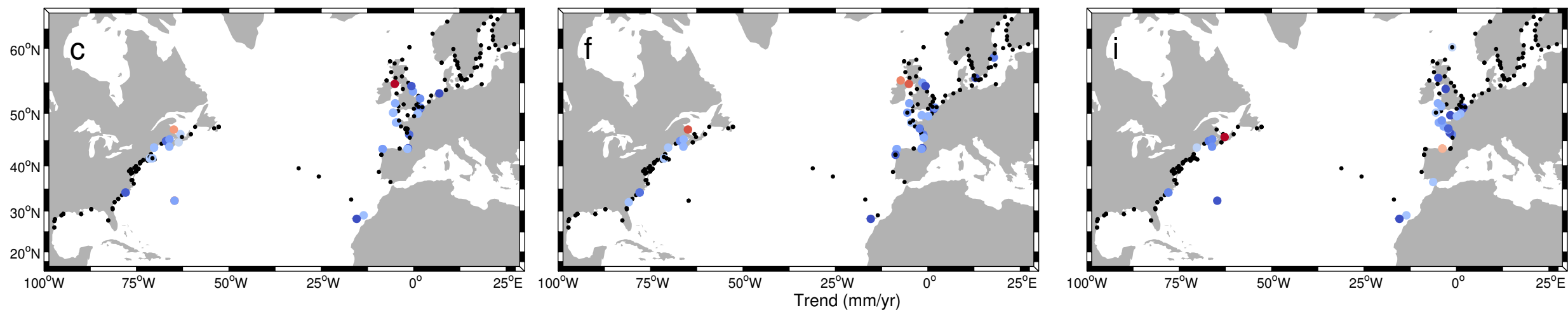
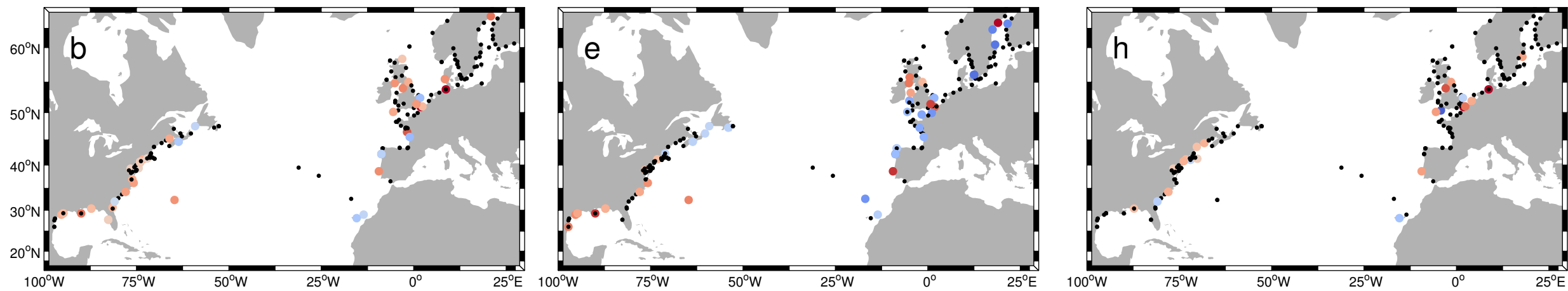
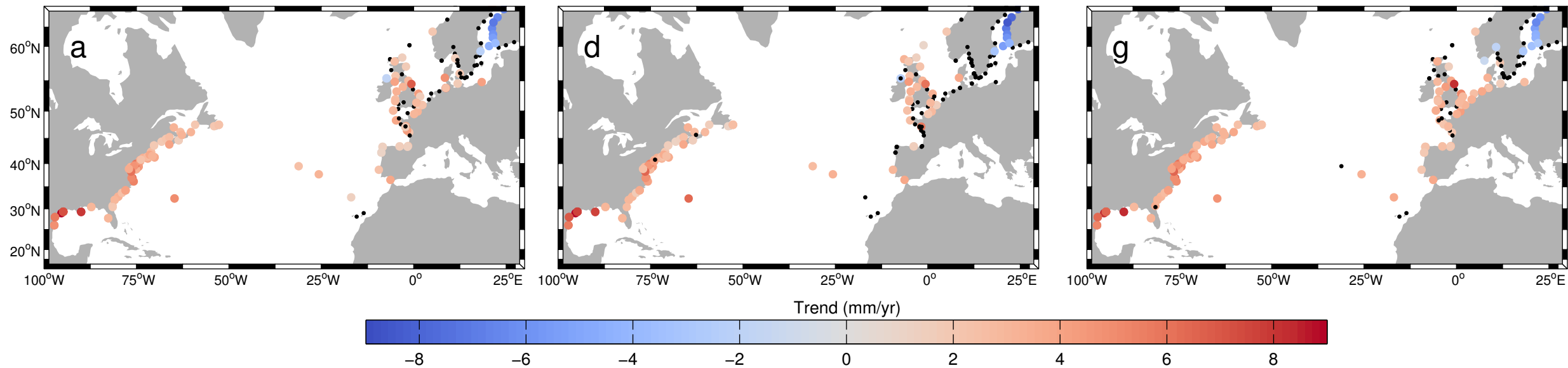
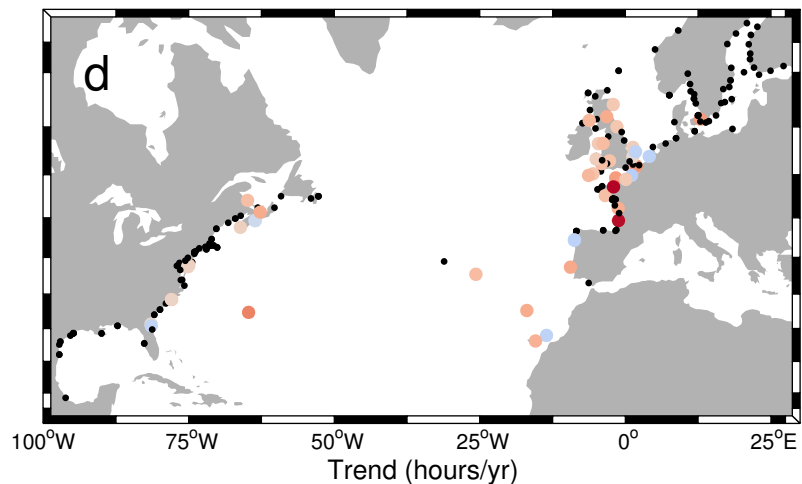
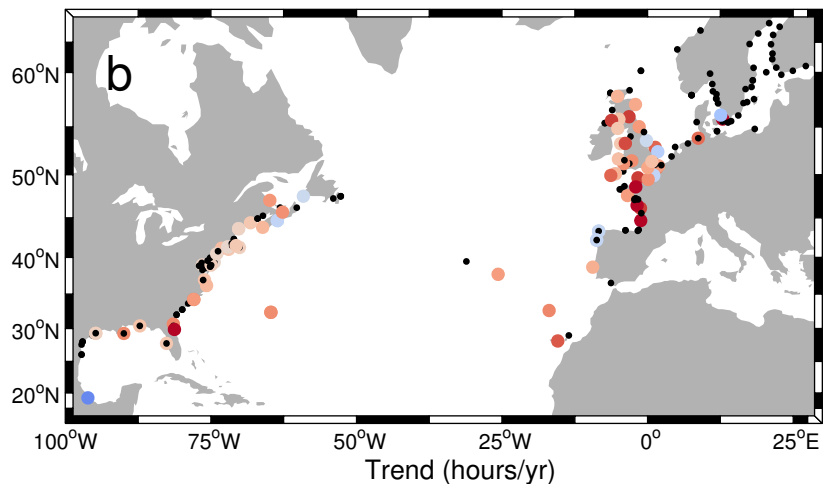
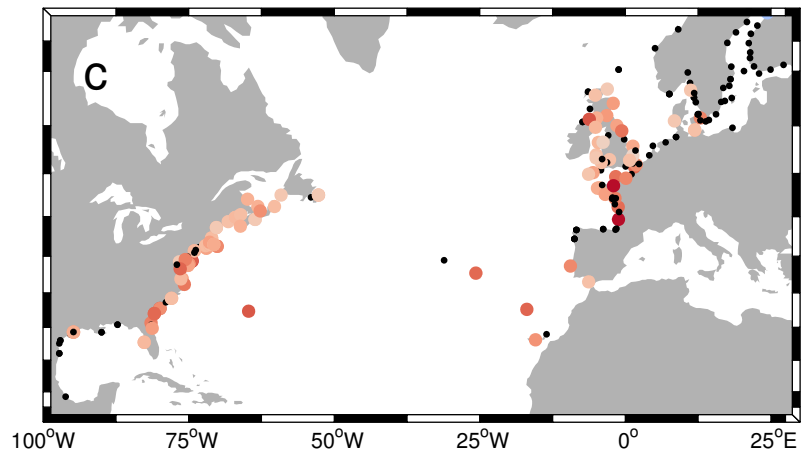
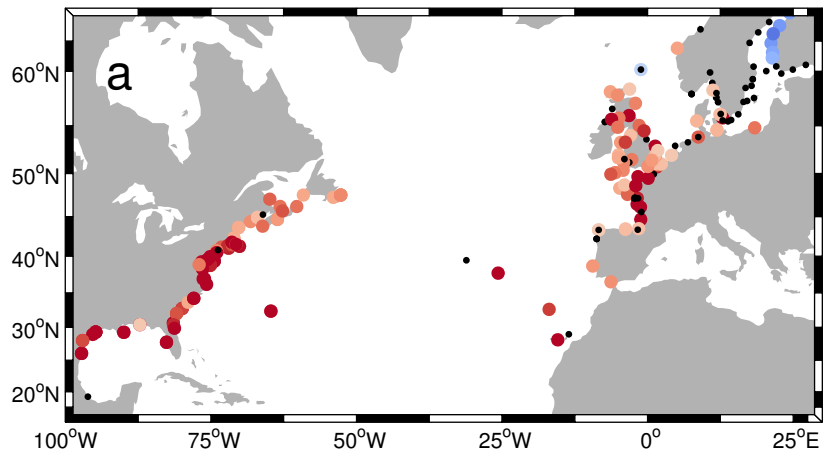
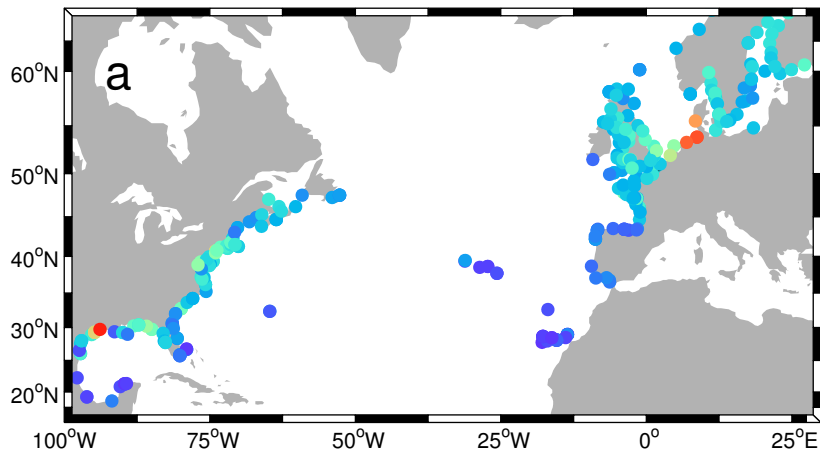


Figure 3.

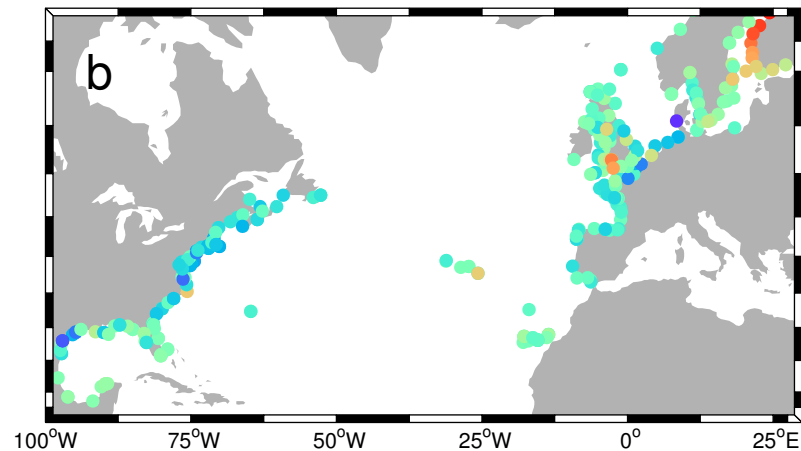
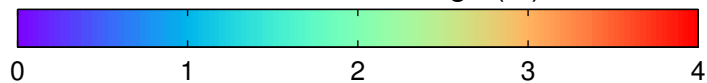
Accepted Article



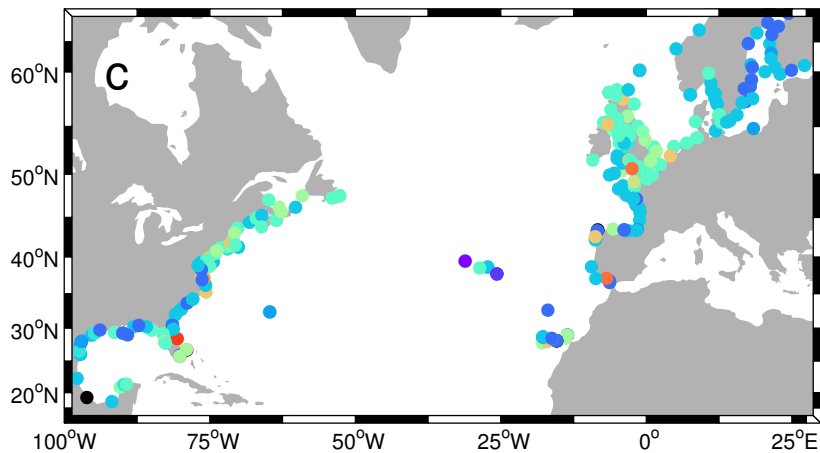
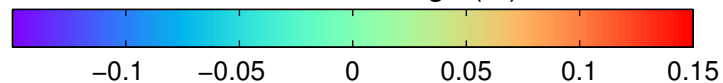
Accepted Article



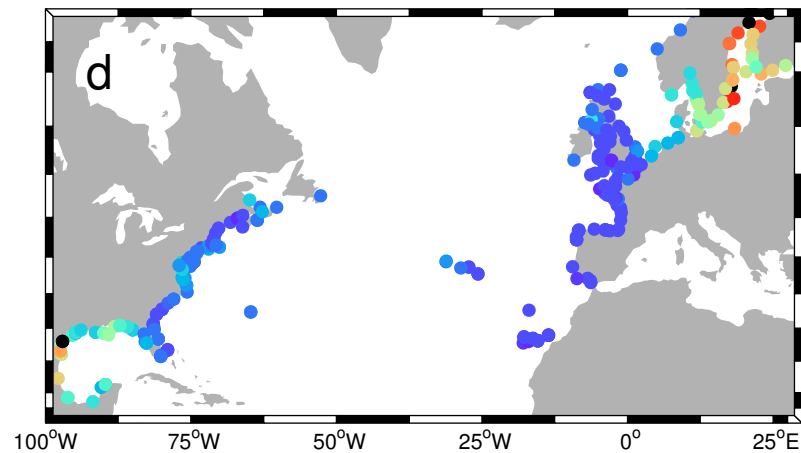
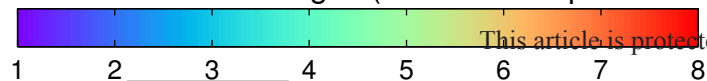
Maximum skew surge (m)



Median skew surge (m)



Median number of surges (over the 99th percentile)



Mean duration (hours)

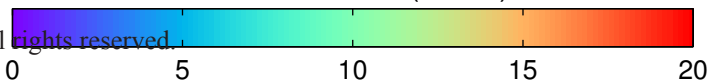


Figure 5.

Accepted Article

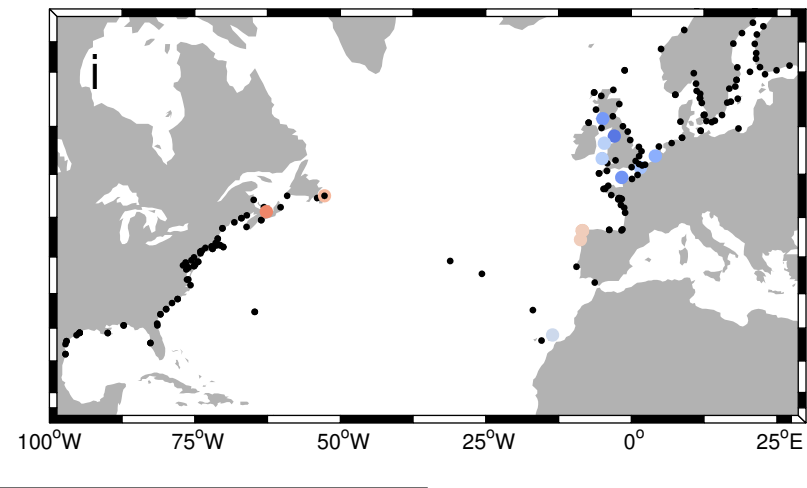
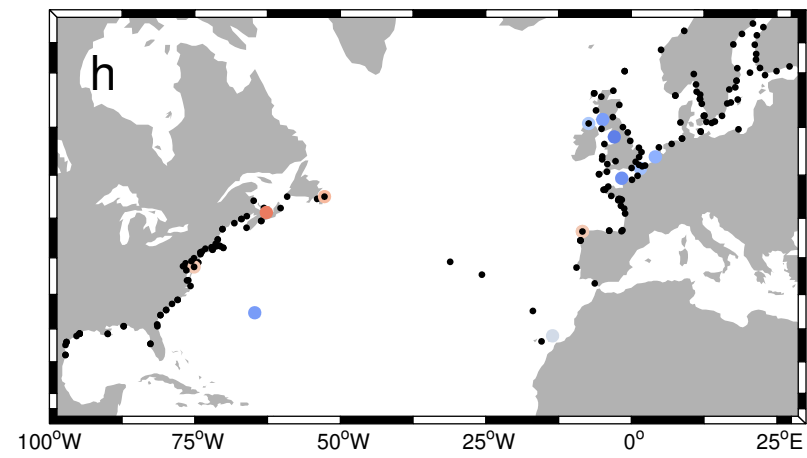
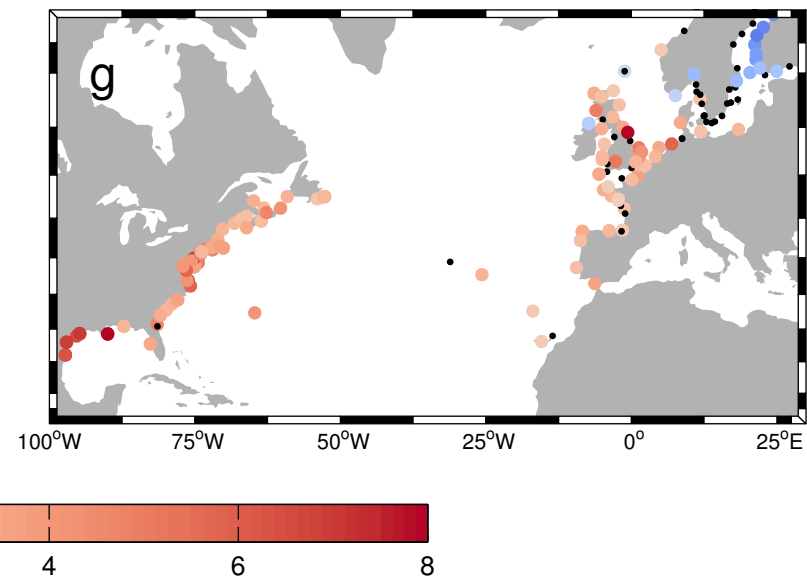
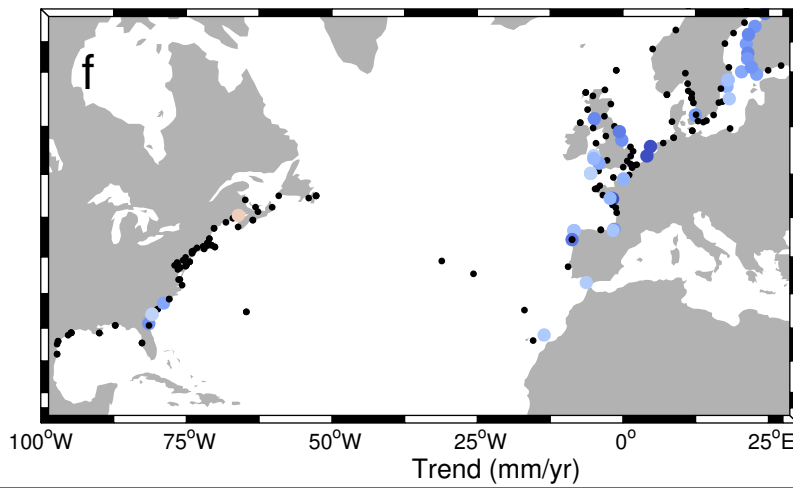
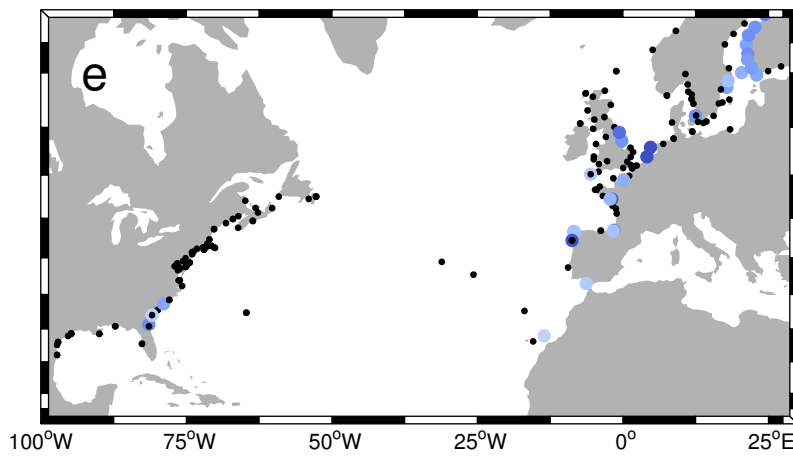
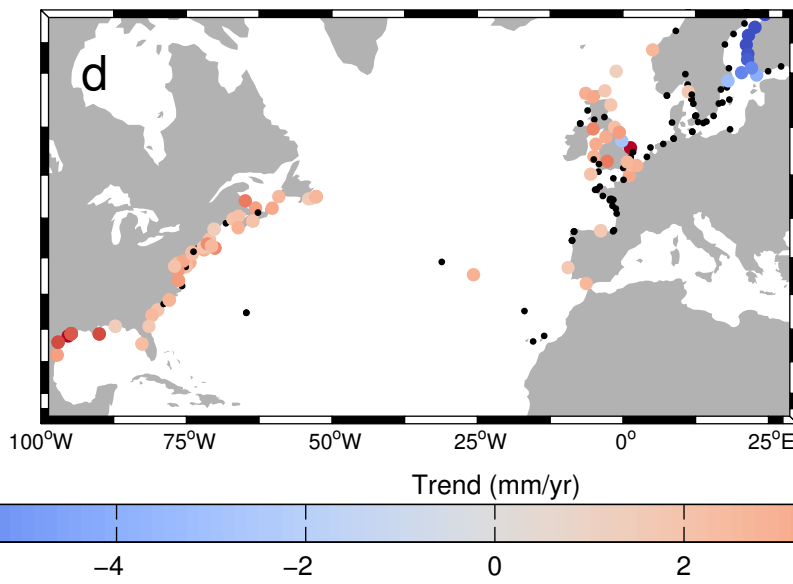
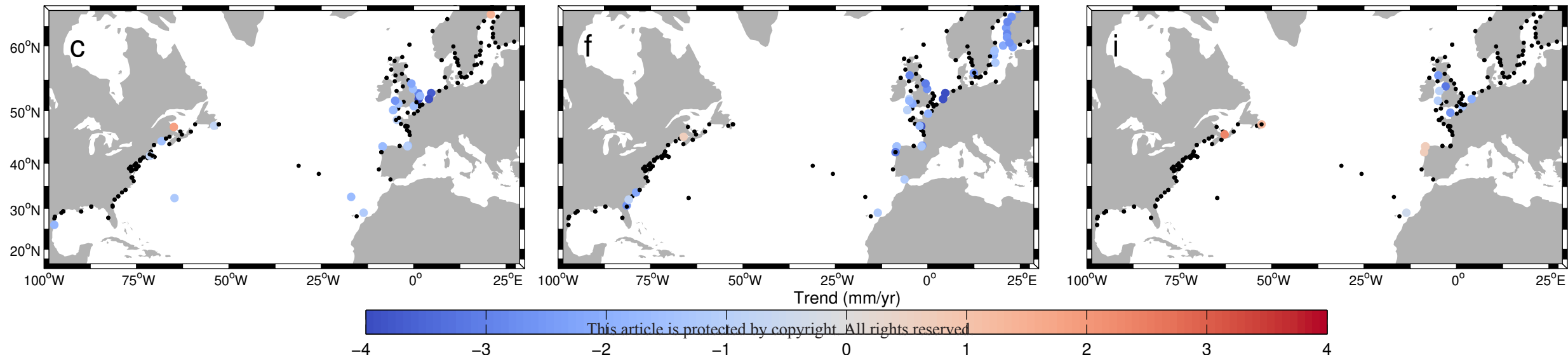
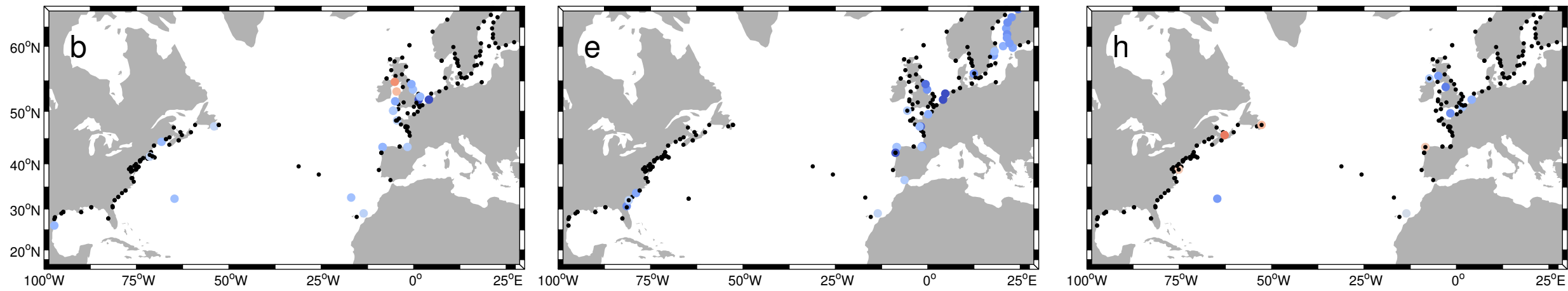
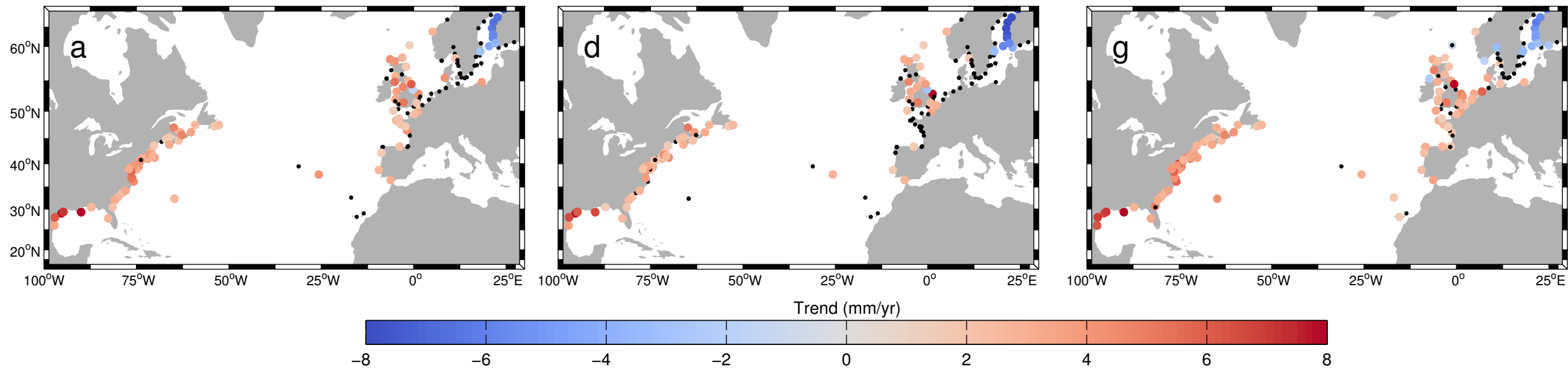


Figure 6.

Accepted Article

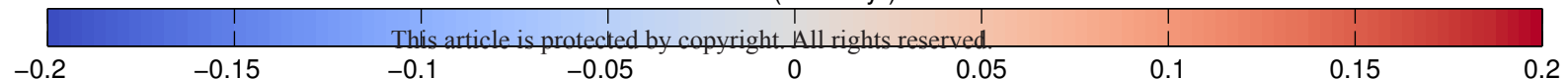
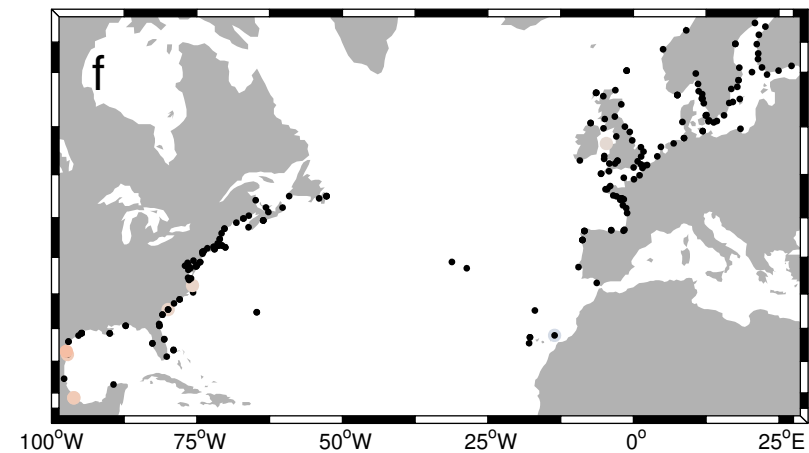
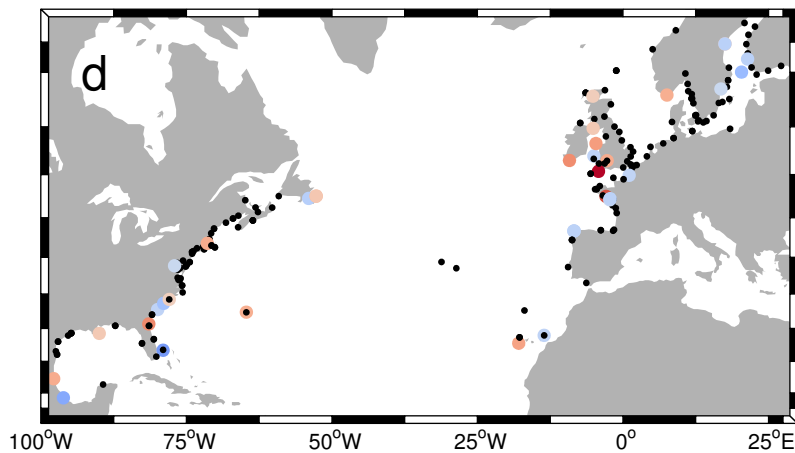
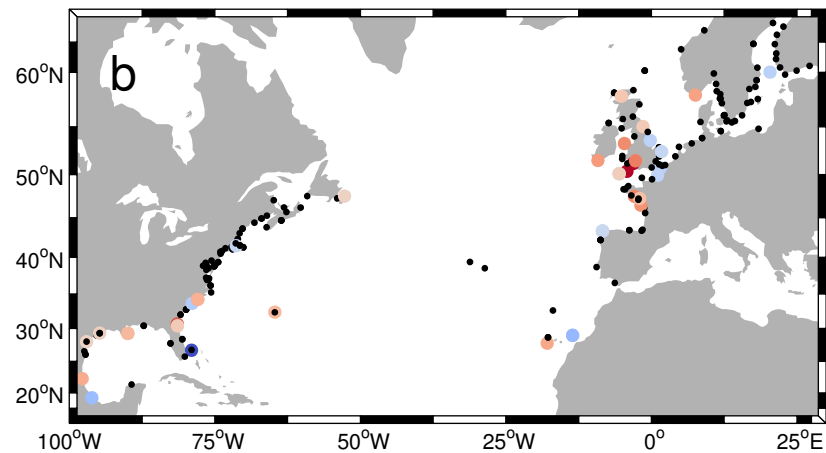
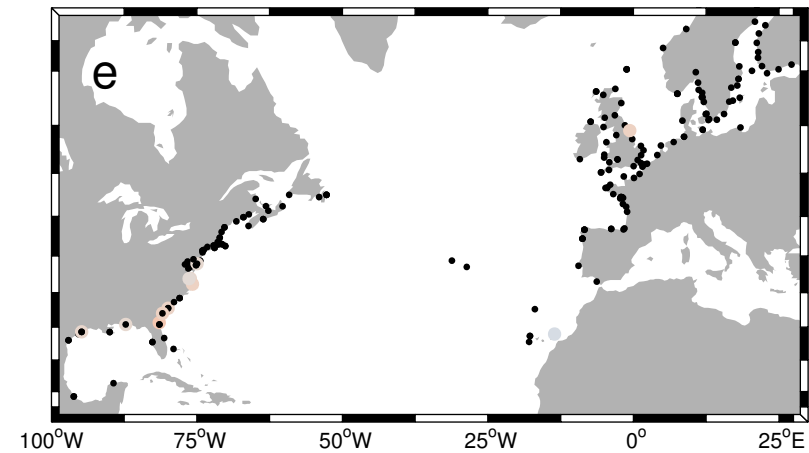
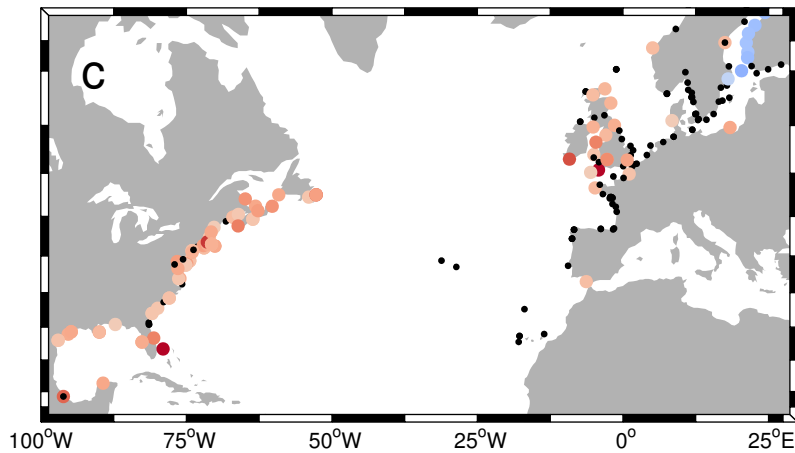
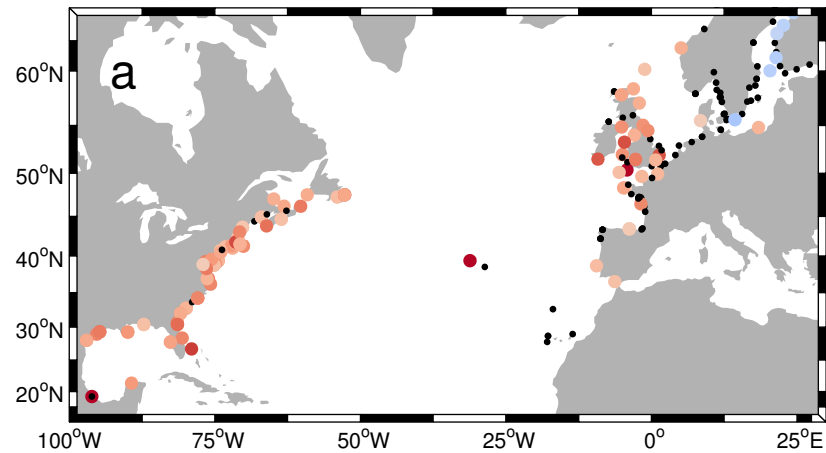


Figure 7.

Accepted Article

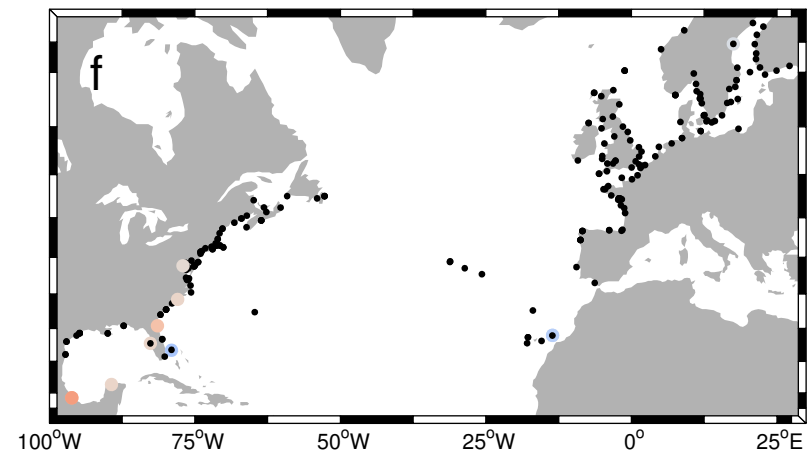
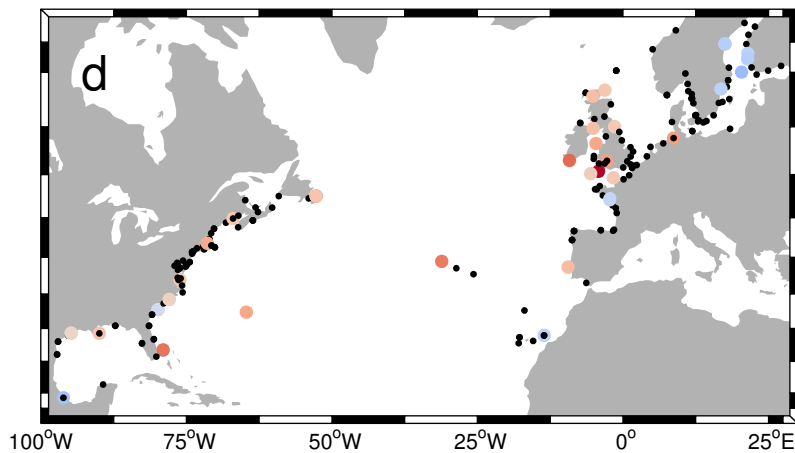
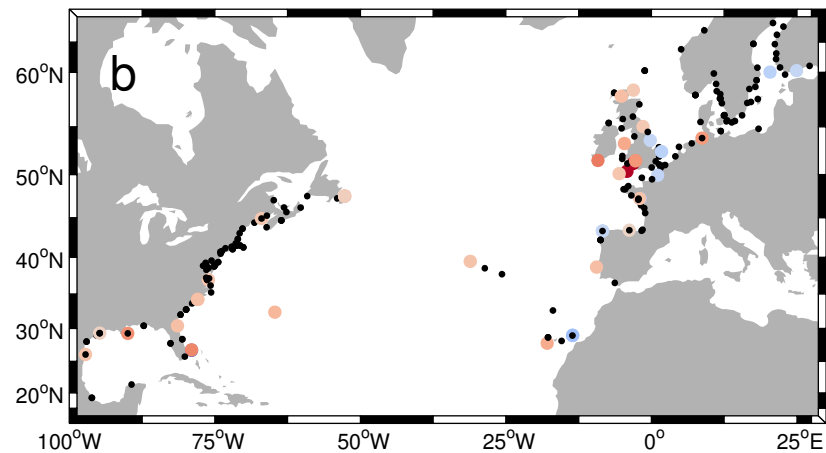
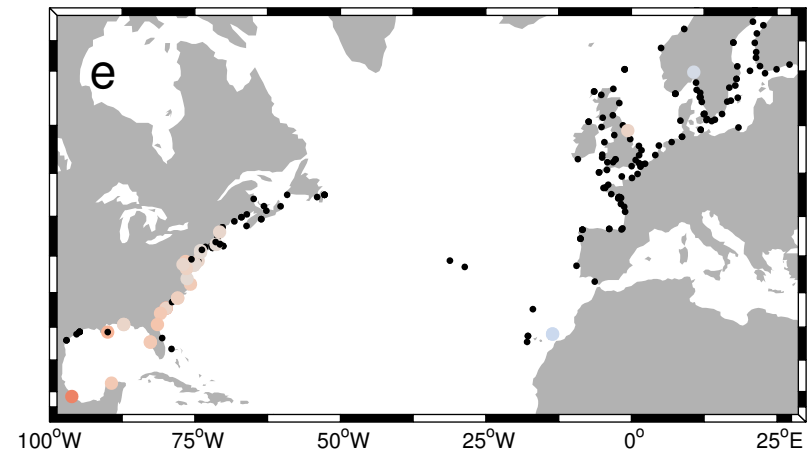
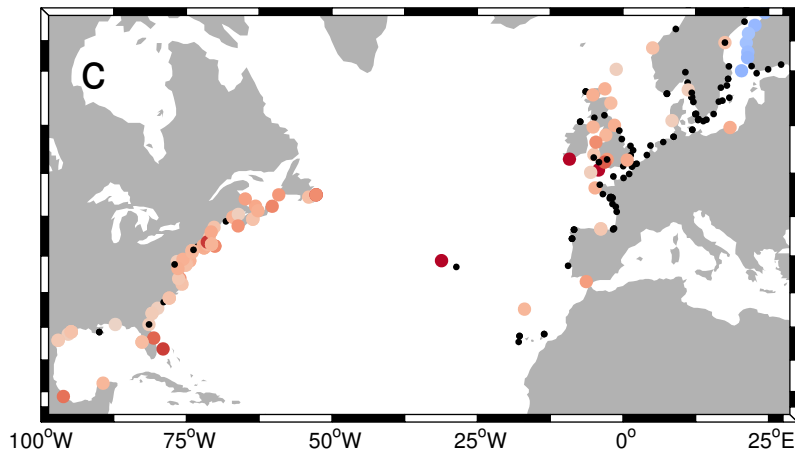
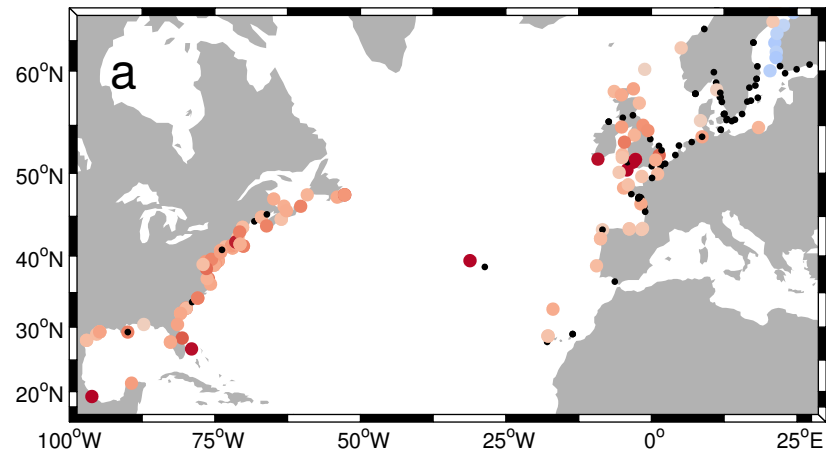
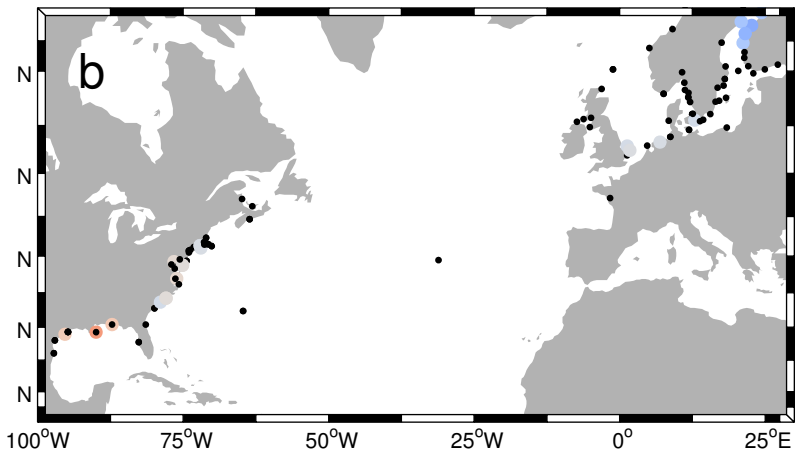
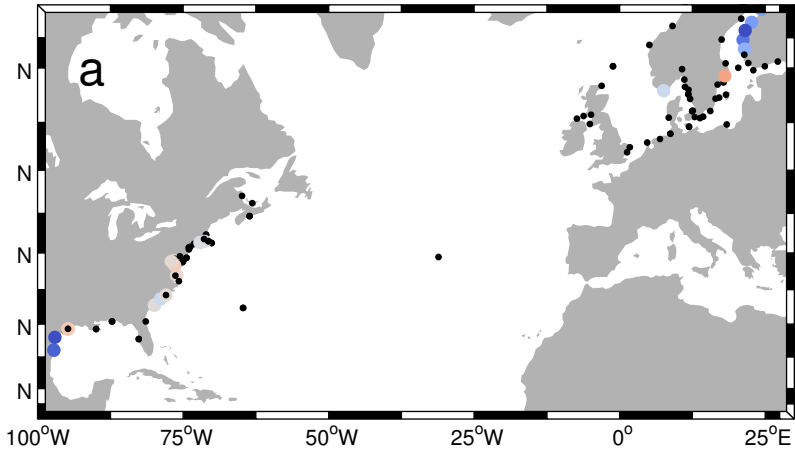
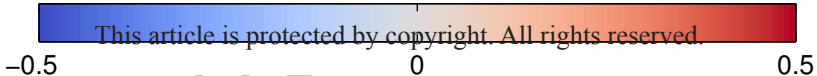


Figure 8.

Accepted Article



Trend (hours/yr)



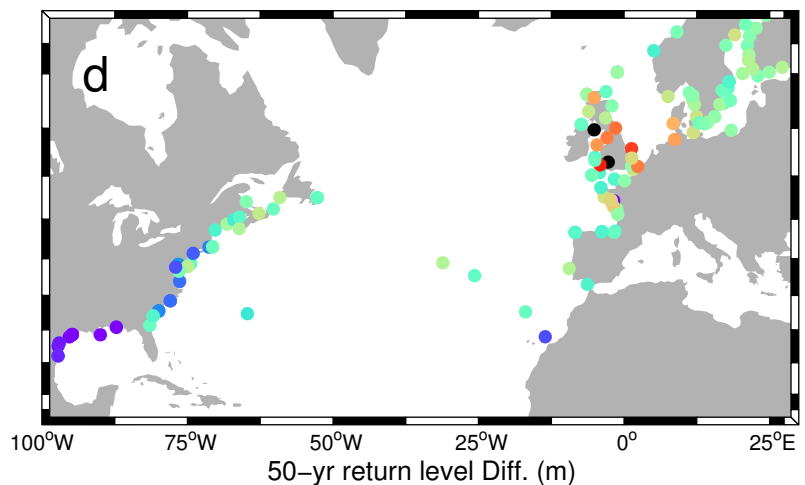
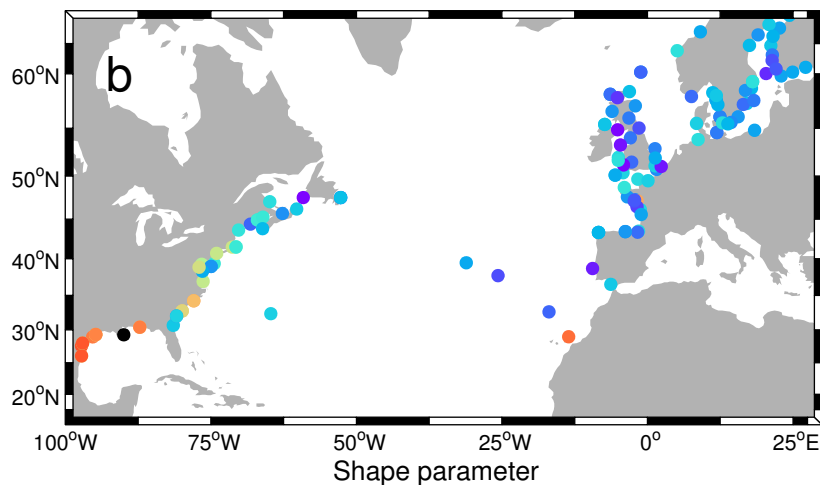
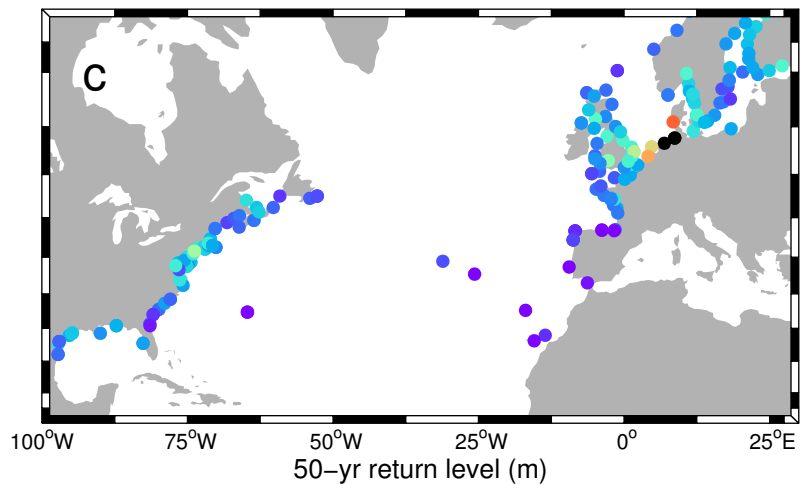
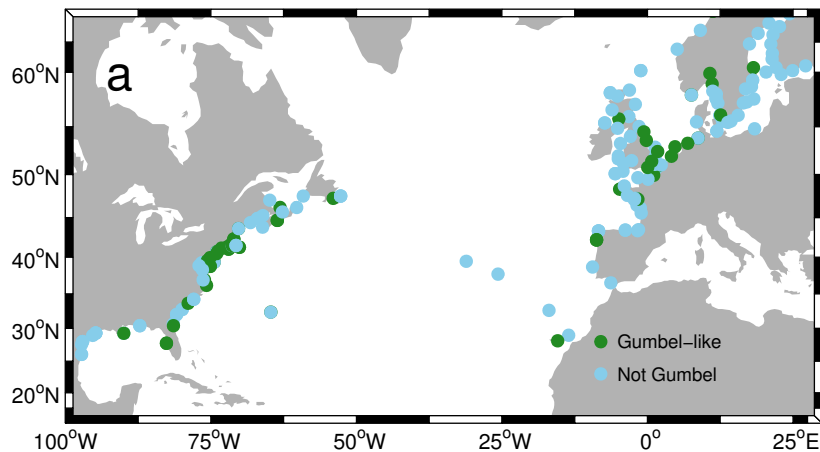
This article is protected by copyright. All rights reserved.

-0.5

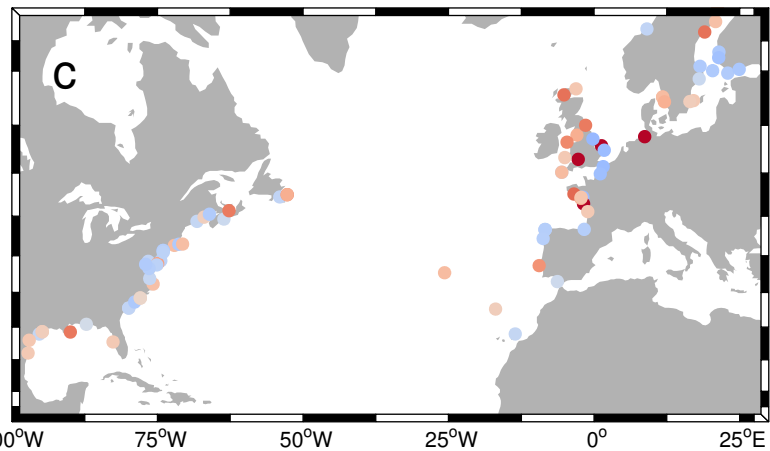
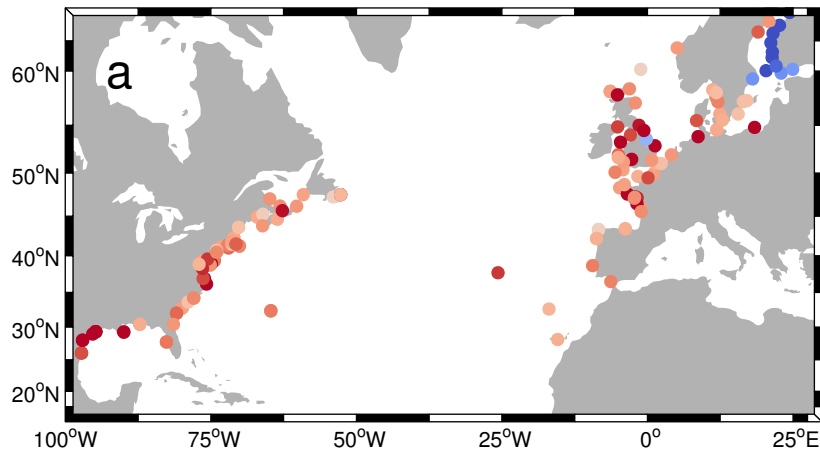
0

0.5

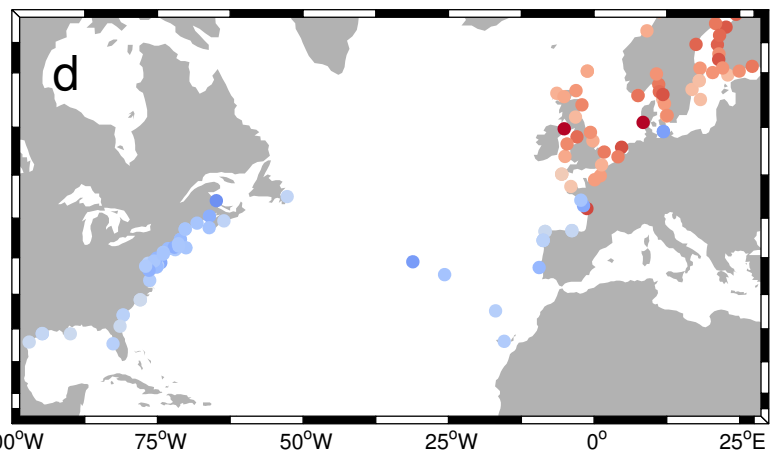
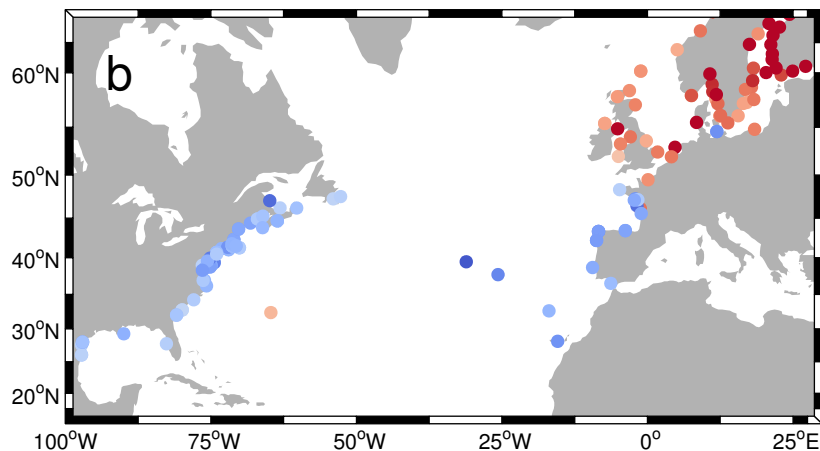
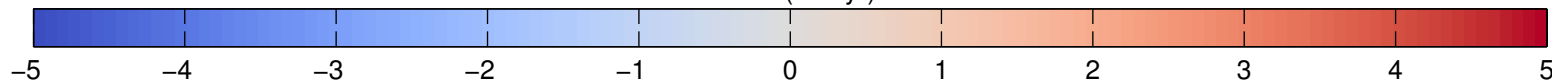
Accepted Article



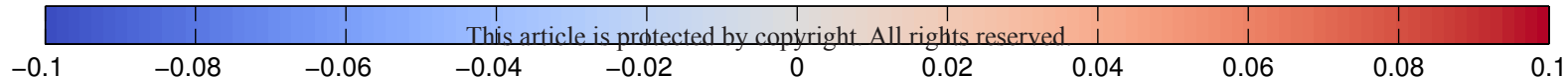
Accepted Article



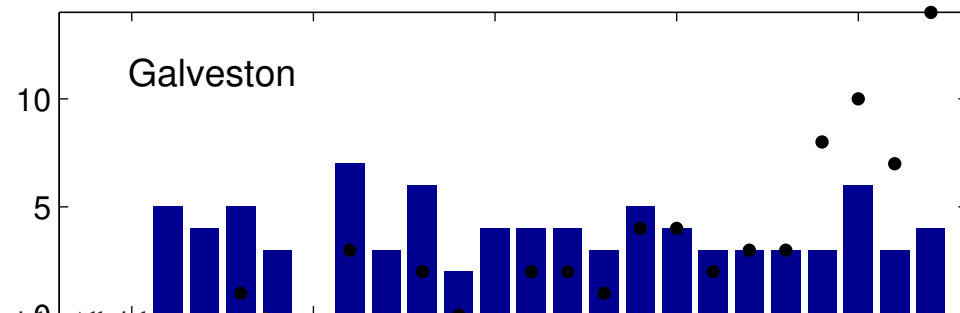
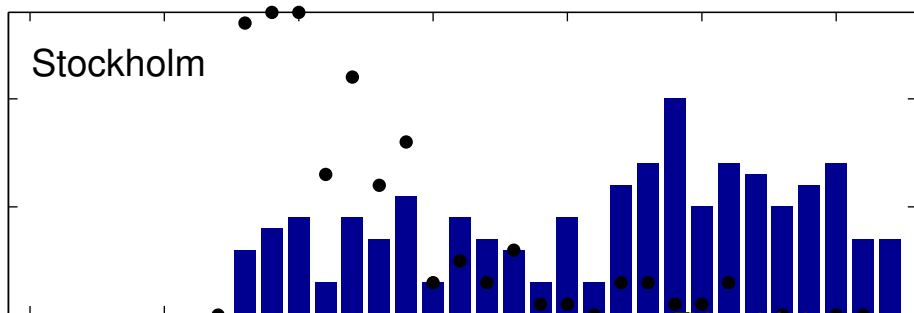
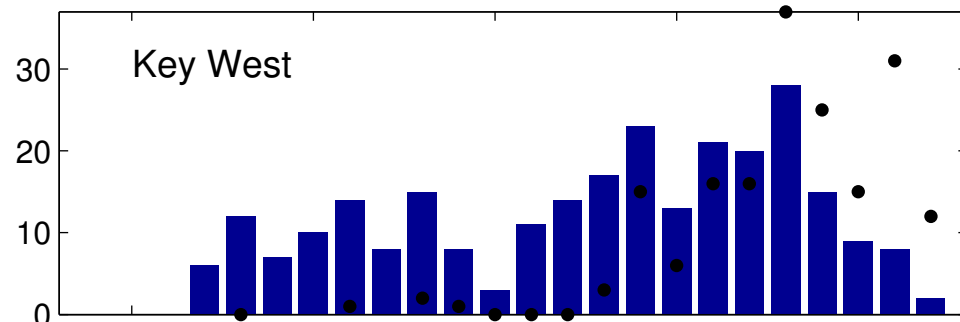
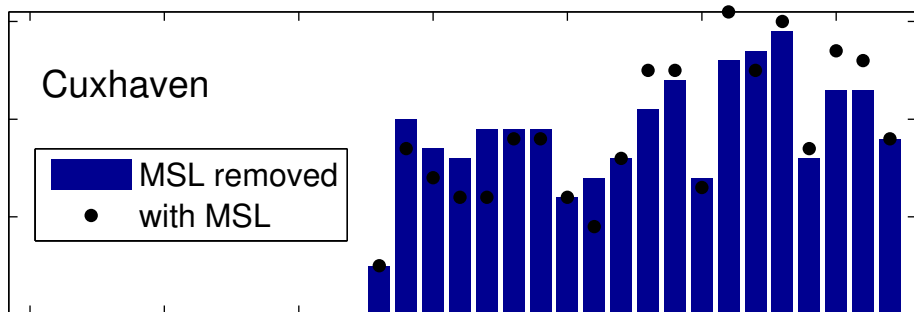
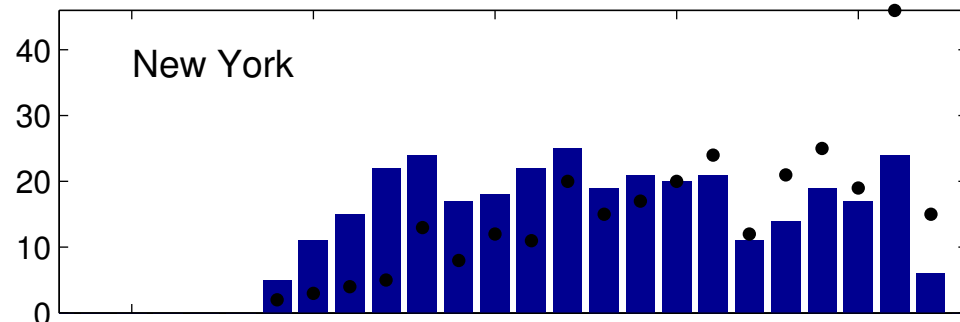
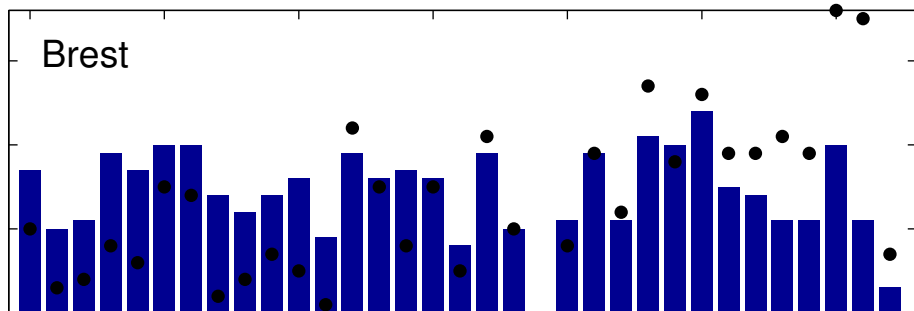
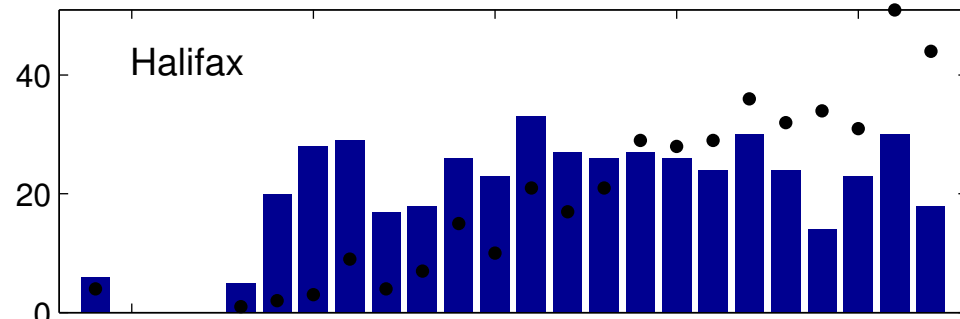
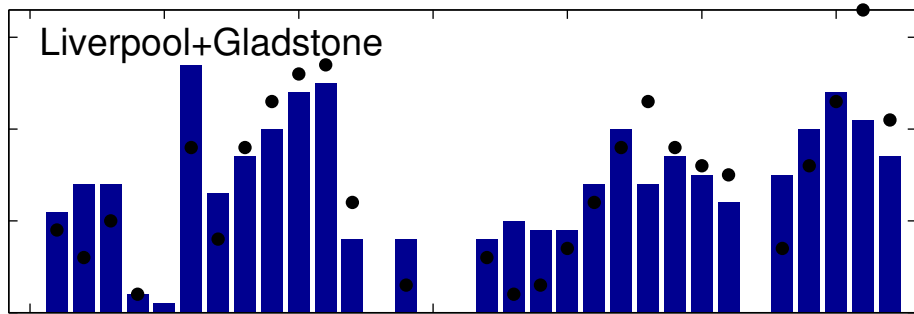
Trend (mm/yr)



m/unit NAO



Accepted Article



Accepted Article

